Project no. 265432

EveryAware

Enhance Environmental Awareness through Social Information Technologies

http://www.everyaware.eu

Seventh Framework Programme (FP7)

Future and Emerging Technologies of the Information Communication Technologies (ICT FET Open)

D1.1: Report on: sensor selection, calibration and testing; EveryAware platform; smartphone applications

---

Period covered: from 01/03/2011 to 31/08/2012
Start date of project: March 1st, 2011
Due date of deliverable: Aug 31st, 2012
Distribution: Public

Date of preparation: 31/08/2012
Duration: 36 months
Actual submission date: Aug 31st, 2012
Status: Final

Project coordinator: Vittorio Loreto
Project coordinator organisation name: Fondazione ISI, Turin, Italy (ISI)
Lead contractor for this deliverable: Fondazione ISI, Turin, Italy (ISI)

Executive Summary

The aim of this project is to raise the environmental awareness of people that in turn will trigger more sensible behaviors. To this purpose it is important to collect data both in terms of subjective and objective measurements, and make people aware of the comparison between what is the sensor measure and what is the personal perception.

The main aim of this document is the description of the work that has been carried out in the **WP1** of the project about the development of the main ICT components for the mobile collection of data about the environmental pollution. For this purpose both hardware and software tools have been implemented in order to make people become a sort of mobile sensing probes. The description of such tools, here in the following called *EveryAware mobile platform*, is the focus of this report. The **WP2** of the project will use the ICT components here described to build the data infrastructure, while **WP3** will deal with the case studies with volunteers and involved communities. **WP4** and **WP5** finally will use and process the collected data to build up the complex system modeling, and following WPs will cover dissemination and management.

Outline of the document

This document is organized as follows. Chapter 1 all the requirements of the EveryAware mobile platform are discussed, while in chapter 2 a description of the air quality sensor selection process of the SensorBox is provided. Chapter 3 describes the SensorBox design and integration and chapter 4 refers to the validation process that has been carried out in order to use the smartphone's microphones for the noise sampling. At the end of the document, the smartphone application is described in details in chapter 5, while all the results obtained in terms of preliminary air quality test results obtained with the mobile platform are depicted in chapter 6.

Contents

List of Figures

Chapter 1

Mobile platform system requirements

This component of the overall system is the equipment available to the users that allows mobile air quality measurements. The block scheme is depicted in Fig. 1.1 where one can see the following components:

- **SensorBox**: this is the system made of custom hardware and firmware that allows the integration of the air quality sensors and communicates with the smartphone through a Bluetooth connection;
- **Smartphone**: throughout a software application, it acts both as data gateway (using standard mobile data connection) and as a local system and user interface;
- **Local User**: it is the user equipped with the mobile platform acting as a mobile sensing probe; other users can just interact with the system through the back-end, and see the output of the data collection;
- **Back-end**: this part of the system collects, elaborates and publishes the collected data; this part is described in the deliverable D2.1.

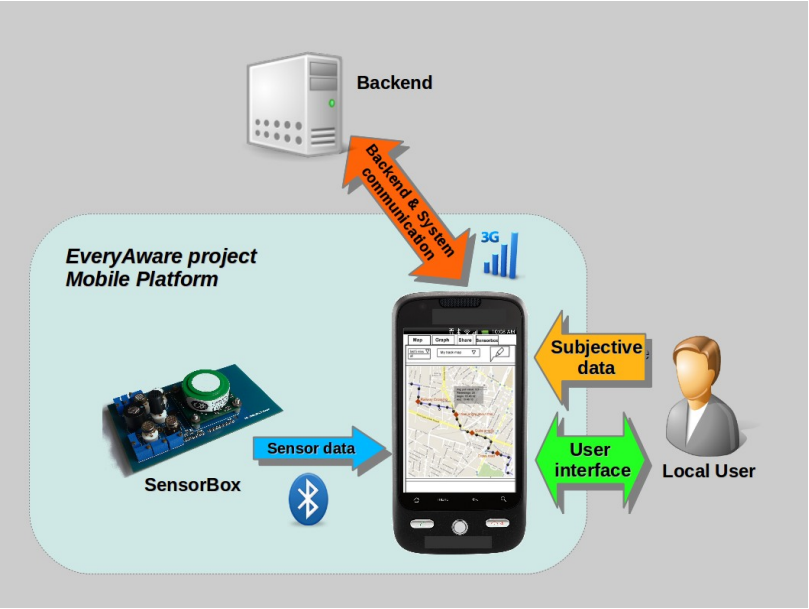

Figure 1.1: EveryAware mobile platform block scheme

Starting from the beginning of the project, the overall architecture of the platform has been continuously discussed among the partners, and some key point have been fixed for the sake of an

optimal result in terms of the usability and scalability of the results.

First of all, *low cost gas sensors* are used in the SensorBox, in order to keep the final production price of the hardware low, and have a larger production capability. The optimal trade-off between sensor price and quality is part of the study of the project, and the results obtained are presented in the current document.

The measurements about *noise pollution* are made using the smartphone's internal microphone: this approach reduces the complexity of the system, and uses a component that is always available in every phone. The main problem of this approach is the possible fluctuations among different kind of smartphones due to different microphones models, calibration and positioning. Part of this deliverable will described the work done to evaluate and tackle these issues.

As far as the *smartphone application* is concerned, two different releases have been developed: The first one is optimized for noise pollution monitoring and does not require a SensorBox. The second one, at the other hand, is build for the detection of traffic pollution and requires the presence of an EveryAware SensorBox. The partners of the project are considering the possibility to merge the two applications. All functionalities required by the project can then be offered by a single application.

The geo-localization of the collected data is done with a *GPS receiver*. After some initial discussions, the partners of the project decided to place a GPS chipset inside the SensorBox, even if modern smartphones are usually equipped with a GPS chipset too. This approach mainly has two positive points: the former is that the SensorBox becomes a mobile data logger that is independent from the smartphone except for the communication with the back-end. The latter is that it is well known that the GPS causes lot of energy consumption, and in the chosen configuration this part of the energy is sinked from the battery of the SensorBox, leaving almost unchanged the battery life of the user's smartphone.

1.1 User interaction

This section describes the requirements for the smart-phone application. The involved elements are: the user, the application and the SensorBox (from which the application obtains actual readings). Before describe the requirements for this application, a number of different type of users has been identified along with theirs limitations, interests and capabilities in the "collective measurement" process. The user interface requirements are a direct consequence of the identified types of users.

1.1.1 Types of users

The following potential "personas" were identified for the air quality test bed:

- cyclists;
- parents bringing children to school;
- commuters.

Even if the application interaction design will be optimized for this kind of users, the implemented intuitive interaction will make it easily usable by anyone.

Cyclists

Cyclists have the mobile phone attached to the handlebar of their bike and when they go past the busy crossing that they are concerned about, they can see the track colored by the current pollution level. They can quickly tap the screen of the mobile to add a marker.

For this kind of user we can identify the following possible interactions:

1. Check the current air quality
2. Mark points of interests along the journey as limited text entry or photograph
3. Record a trip for later further analysis via a web application

The whole point of the application is to make it quick and unobtrusive to use while traveling. It would be useful if the application could allow the cyclist to use the map for navigation purposes. The focus is on the journey, which starts when the application is turned on and stops when the user closes it. The application keeps the track for the journey and allows the user to add annotations (e. g. text or photos) as markers (way points) along the track. All further analysis, review and annotation is left to the web application interface, on a second time (e. g. when the user comes back home).

Parents bringing children to school

They undertake a repeated journey every day to and from the school. Also, the time is the same and depends on the school open/close schedule. Each mother or father may be accompanied by one or more children of school age, but also by one or more children younger than school age, who may be in a buggy. Once at the gates to the school, they meet each other. They may go for coffee with their friends after they have dropped the children off. This kind of group is interesting because it can collect a repeated set of measures for the given track, that can be used to analyze the evolution of air quality over the time. For this people, the primary focus remains watching young children, also they may have buggies, shopping and other limitations. The primary feedback (and motivation to collect such kind of information) is to understand their level of exposure with an immediate and meaningful way, also they may be interested in the differences of exposure compared to their children (due to the differences in the heights). Mother and fathers may be interested to compare their readings with each other.

Commuters

Commuters make the same journey to and from the place of work every day. The journey may be made using public transport such as buses, trains or metro (underground) systems. As the “group of parents” this kind of workers can collect a repeated set of measurements for the given track twice per day, allowing both time/space comparison. Their travel may involve underground journeys, when both phone and GPS signal could be lost. The main interest is to identify the exposure and how it can be modified with different routes or choices in transport system. As in the case of the group of parents, workers may want to compare and share their recordings with colleagues (during coffee breaks for example).

1.1.2 Interface design

In general the application should use the track metaphor which is like the GPS metaphor. So a track is the journey one person took which is created when a person turns the device on and ends when the device is switched off. Along the way the user can add markers (waypoints) which are textual or photographic and which can be further annotation via the web interface. The user should be shown a map of their data when the application is started. This will show their current location but will also allow them to move back in time and/or select on their data and add annotations. The annotation should be provided as free text and/or a selection of push buttons.

The user may configure the push system by setting the number of notifications per day or by limiting the reception of this message only in a given zone or time. Push notification should be signaled using standard alerting systems used by telephony application (e. g. vibration and or sound). As happens for any other notification the user may answer after a while or just ignore it.

The trace on the map is colored depending on the readings, using a scale of 5 categories. The user should be able to annotate points on the data graph too - especially to handle the situation where the sensor box is in one location for a long period of time. A clear explanation should be given of the categories as far as possible (e. g. "this reading equates to standing behind a bus for 5 minutes"). Manual correction of GPS position may be made available to the user during the annotation phase.

The interface should provide access to the following views:

map - the main map as already described;

share - where the users can tweet results or share them to Facebook;

about - where the application gives the link to the webpage for the project, and further details of the developers;

more info - where users can receive contextual information about the values they are seeing, as well as links to web pages and/or annotate previous data;

configuration - where the application allows user registration and modify push settings;

graphs - where user can take a look to graphs of the readings (or other means of reporting).

The type of users taken into consideration in general must keep their attention to other tasks and may not be able be able to produce a continuous data stream. To avoid this the interface may implement a "push model" where the system itself prompts the user to provide its feedback or annotation. This request may be triggered by different events:

- when the user is in a fixed location for given period (e.g. a coffee shop);
- at certain times of day;
- when certain events occur (e.g. a parameter is outside a given range);
- when user is walking inside a geographic location of interest (bounding box).

Where positional information is not available for data points (as the user has been underground) two options should be considered:

1. to present the user a different "layer" that draws a line between their last known GPS position and then the GPS position when they emerge from the underground; the data is then attached to this line in proportion to the time it has taken them to traverse the route;
2. to present the data as a point on the map where the GPS signal disappeared / emerged; by clicking on this point will take them to a graph showing the data for the time there was no location information.

1.2 SensorBox air quality sensor requirements

In urban areas air quality is highly related to traffic. According to the latest report of VMM [Vlaamse Milieumaatschappij, 2009], transport in Flanders is responsible for 61% of the emission of NO_2,

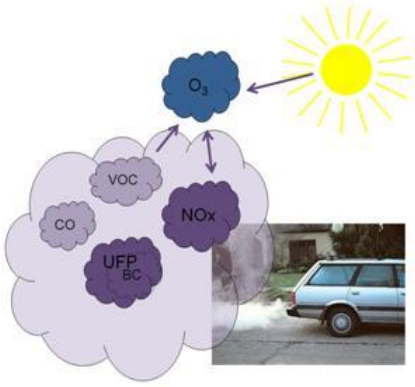

Figure 1.2: Traffic pollution is a complex mixture of gases

30-40% of the emission of particulate matter and it causes 42% of the potential tropospheric ozone emission.

Especially in urban environments traffic contributes disproportionally to human exposure to air pollutants, as these pollutants are emitted near nose height and in close proximity to people [Dons et al., 2011] [World Health Organization, 2000].

With the EveryAware SensorBox, we want to offer an affordable measurement device which allows citizen scientists to detect the presence of traffic pollution in urban environments such as Antwerp, London and Rome. A trade-off between sensor quality and price will be required. This should not compromise the reliability of the measurements too much.

In this subsection, the requirements are identified for the air quality sensors to be used in the EveryAware SensorBox.

1.2.1 Best fitted air quality components to measure

The EveryAware SensorBox should be able to inform the citizen scientist about the presence of traffic pollution. Traffic pollution is a complex mixture of gases, such as nitrogen oxides (NO, NO_2), carbon monoxide (CO), volatile organic compounds (VOC), and fine and ultrafine particles (UFP) (Figure 1.2). In this section we will identify the traffic pollution components which are most promising for the EveryAware SensorBox to measure.

The best indicators of the presence of traffic pollution are those air pollution components that leave the vehicle tail pipes in a relative large amount compared to the concentrations already present in natural background, and for which no other major sources are present in the urban atmosphere. Ultra Fine Particles (UFP), Black Carbon (BC) and the smallest fraction of fine dust (PM1) are known to comply very well to this requirement [Morawska et al., 1998] [Harrison et al., 2011] [Pey et al., 2009] [Janssen et al., 2011]. None of those traffic pollution components can be measured directly by the EveryAware SensorBox since, to our knowledge, no UFP, BC or PM1 sensor is available on the market for less then 500 Euro. For this reason, the EveryAware SensorBox will be equipped with a number of low cost gas sensors to measure traffic pollution. The following table gives an overview of the most interesting gas components in traffic pollution with an indication of their typical concentration at the tail pipe and in ambient air in urban environments.

In the table above Nitrogen Oxide (NO) has the most distinguished ratio between tail pipe concentration and ambient air concentration in urban environments. On the second place comes Carbon Monoxide (CO). The ratio for Nitrogen Dioxide (NO_2) is less distinguished directly at the tail pipe. In practise the measured NO_2 concentrations in traffic pollution are much higher due to the fast reaction of Nitrogen Monoxide with Ozone (O_3) to form Nitrogen Dioxide.

The amount of Carbon dioxide (CO_2), Oxygen (O_2) and water (H_2O) in the tailpipe exhaust differs

Table 1.1: Typical concentrations of gas components at vehicle tail pipe, in natural background air and the tail pipe / background air concentration ratio

Gas component	Tail pipe conc. (ppm)	Natural backgr. air conc. (ppm)	Tail pipe / Backgr. air conc. ratio
H_2O	70000	20000	3,5
CO_2	70000	390	180
CO	1000	0,4	2500
NO	300	0,001	300000
NO_2	35	0,02	1750
O_2	-50000	209000	-0,239234

tens of thousands of Parts Per Millions (PPM's) from the concentrations in ambient air. Still, we do consider those gases less fitted for the detection of traffic pollution because of the quite high concentrations of those gases already present in natural ambient air. The tail pipe / natural ambient air concentration ratio is significantly less distinguished for CO_2, O_2 and H_2O as for CO, NO and NO_2.

Volatile Organic Compounds (VOC), and more specifically hydrocarbons (HC) are also present in traffic pollution and could have potential. Hydrocarbons are produced by incomplete combustion of hydrocarbon fuels. No concentrations of HC and VOC are given in Table 1.1 since they are many hundreds of different compounds [Juszkiewicz and Kijak, 2003]. HC and VOC sensors typically react on a subset of different HC or VOC compounds. This makes it quite hard to evaluate, from a theoretical point of view, how well they are fitted.

We can conclude Nitrogen Oxide (NO), Carbon Monoxide (CO) and Nitrogen Dioxide (NO_2) are the best fitted gases to measure to detect the presence of traffic pollution. HC and VOC sensors may also have potential.

1.2.2 Crucial sensor requirements

All gas sensors need to meet following minimal requirements to be considered for usage in the EveryAware SensorBox.

Low cost: Citizen scientists have to be able to afford the EveryAware SensorBox. For this reason, only gas sensors with a relative low price can be used in the EveryAware SensorBox.

High sensor sensitivity: To measure concentrations of traffic related air pollutants in ambient air requires very sensitive measurements, even at heavy traffic locations. For CO the concentrations are typically in the 0.2-5 ppm range. For NO and NO_2 the concentrations are typically in 20-500 ppb range. Only gas sensors can be considered which are able to detect those very low gas concentrations present in ambient air.

High temporal resolution: The EveryAware SensorBox should be able to support mobile air quality measurements. Due to the high spatial variability of air quality in urban environments, the EveryAware SensorBox will be exposed to quick changing pollution levels. We want to be able to read out the air quality sensors with a high temporal resolution (around 1 Hz) to map the spacial variability of air quality.

1.2.3 Additional Sensor requirements

The ideal gas sensors for the EveryAware SensorBox should meet a number of additional sensor requirements. Since the ideal gas sensors are not available on the market compromises are required and choices will have to be made (Section 2).

Figure 1.3: Typical Geiger tubes

No sensitivity to meteorological influences: The gas sensor signal should not be influenced by changes in temperature and humidity. Also the presence of wind and exposure to the sun should have no influence on the measurement result.

Low power usage: Since the EveryAware SensorBox is powered by a battery, the power usage of the used gas sensors should be as low as possible to extend the autonomy of the measurement device.

Short stabilization time after power on: When powered on, low cost gas sensors typically require some time before they are able to deliver a stable sensor signal. We will discuss the further in the next chapter on low cost air quality sensors (Chapter 2). The shorter the stabilization time of the sensor, the faster the user can start using the measurement device after powering it on.

Fast reaction time: Low cost gas sensors need some time to react on changes in the gas concentration to measure. The faster the gas sensor signal is able to react, the better. Also, some time is needed to allow the sensor signal to stabilize again after the change. Here to, faster is better.

Weather proof: We want to be able to conduct air quality measurements under all weather conditions: during rain, sun, cold winters and hot summers. The sensors, in combination with a fitted sensor housing, should allow this.

No cross sensitivity: The used low cost gas sensors should only react on changes in the concentration of the gas they are supposed to measure. Changes in the concentrations of other gases should not influence the measurement signal of the gas sensor.

No baseline drift: The sensor baseline signal should be stable over time.

No sensor aging: The sensors should not be sensitive to sensor aging. We don't want the sensitivity of low cost gas sensor to decline over time.

1.2.4 Geiger sensors

The last dramatic nuclear environmental alarm that followed the tsunami on March 11th 2011 in Fukushima (Japan), triggered among common people a larger awareness with respect to the problems related to the use of atomic energy for civil purposes. Decision makers were then forced by public opinion to revise the energy strategies of their countries: in Italy, after a popular referendum held in June 2011, more than 94% of voters opposed the government's plans to resume nuclear power generation, while in Germany as well as in Japan it was decided to gradually dismiss the existing nuclear plant network.

For this reason, riding the wave of social concern, we studied the possibility of introducing a Geiger sensor in our SensorBox. Traditional Geiger sensors consist of elongated tubes containing a gaseous substance. When an ionizing radiation enters the tube, an electrical discharge is produced and the current flow is measured. Thus, the measured current intensity is directly related

to the number of ionizing particles going through per unit time (radiation). Unfortunately these sensors require a relatively high voltage to be operated: from 400 V up to 800 V for some models. While the typical currents are very low and result in a negligible direct energy consumption, those high voltages pose serious design bounds, being the necessary circuitry to produce those voltages rather cumbersome and critical for electromagnetic compatibility issues. Moreover, after the Fukushima disaster, the high demand of Geiger sensors resulted in a substantial price rising up to 10 times the original price (from 15$ to 150$). Therefore, because of high price (remind we aim at designing a cheap sensor box) and design issues, we decided to explore new technologies of radiation sensors. Recently, we came across a made in Japan device [Radiation watch] using photodiodes to detect gamma rays radiations. According to the selling company, with an array of 8 tantalum photodiodes [Vishay VBPW34 photodiode] (today prices around 3$ each) it is possible to detect radiation intensities ranging from 0.05 μSv/h to 10 mSv/h (one set of dental radiographs corresponds roughly to 5 μSv). We are now exploring the feasibility of inserting this kind of devices in our SensorBox.

Chapter 2

Low cost air quality sensors for the EveryAware SensorBox

2.1 Sensor operation principles

Low-cost sensors are commercially available for NO_2, NO, CO, and VOC. However, few of them are intended to be used in the ppb-range that is relevant for urban air quality. Most commercially available sensors are built with other applications in mind, e.g. for safety applications such as detecting CO poisoning. Most commercial available basic gas sensors for NO, CO, NO_2, and VOC are metal oxide sensors or electrochemical sensors. This section gives a short overview of their operation.

2.1.1 Metal oxide sensors

Semiconductor metal oxide sensors consist of one or more oxides from the transition metals. Commercially available gas sensors are mainly made of SnO2 in the form of porous pellets or thick or thin films deposited onto an alumina or silica substrate. The sensing properties are based on the reaction between the semiconductor metal oxide and oxidizing or reducing gases in the atmosphere which lead to changes in conductivity. This change in conductivity is measured over a pair of interdigitated electrodes embedded into the metal oxide (see Figure 2.1). A (mostly platinum) heating element is used to regulate the sensor temperature. The sensors have to be heated to 200 till 400 degrees Celsius to increase sensitivity and decrease response time. They exhibit different gas response characteristics at different temperature ranges. Selection of the best operational temperature for each specific gas enhances the sensitivity and minimizes the cross sensitivity. Sometimes thin layers of other metal (e.g. gold nano-particles) or metal oxides are deposited on the sensing layer to act as a catalyst or a filter. The cross sensitivity of the metal oxide sensor can be reduced by adding filters. Examples are ozone scrubbers added to some NO_2 sensors, and charcoal filters added to some CO sensors.

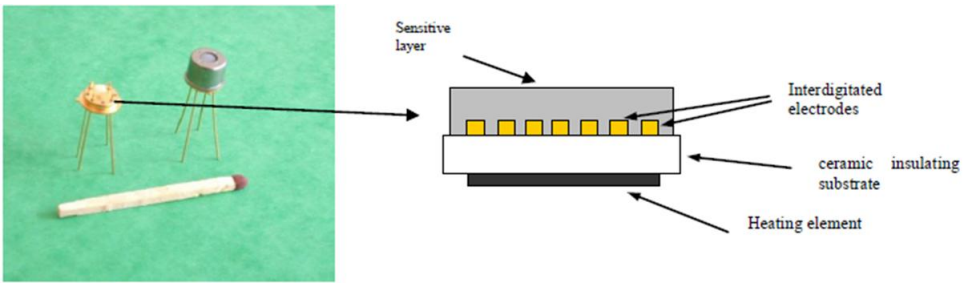

Figure 2.1: Schematic metal oxide gas sensor

2.1.2 Electrochemical sensors

Electrochemical sensors operate by reacting with the gas of interest and producing an electrical signal proportional to the gas concentration. Figure 2.2 gives an overview of the schematics of a typical electrochemical sensor. The sensor consists of a sensing electrode (also called working electrode), and a counter electrode separated by a thin layer of electrolyte. Gas that comes in contact with the sensor diffuses through a hydrophobic solid polymer membrane, eventually reaching the sensing electrode surface. The sensing electrode either oxidizes or reduces the target gas with the counter electrode balancing the generated current. These reactions are catalyzed by the electrode materials specifically developed for the gas of interest. However, the sensing electrode potential does not remain constant due to the continuous electrochemical reaction taking place on the surface of the electrode causing a deterioration of the performance of the sensor over an extended period of time. Consequently, a reference electrode is placed within the electrolyte in close proximity to the sensing electrode. The reference electrode anchors the working electrode at the correct bias potential. The value of the bias voltage applied to the sensing electrode makes the sensor specific to the target gas. With a resistor connected across the electrodes, a current proportional to the gas concentration flows between them. The current can be measured to determine the gas concentration. Because a current is generated in the process, the electrochemical sensor is often described as an amperometric gas sensor or a micro fuel cell. When gas concentrations are measured in the ppb range, the generated currents can be as small as a few nano-amperes.

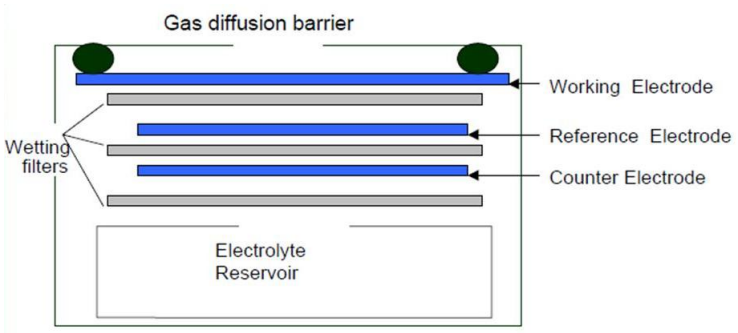

Figure 2.2: Schematic electrochemical gas sensor

2.2 Sensor properties

In this section, an overview is given of the key properties of low-cost gas sensors.

Sensor electronics: Electrochemical sensors require 2 functions from their sensor electronics. First of all they require 'potentiostats' to ensure the potential difference between the measurement electrode and the electrolyte stays constant . Figure 2.3 shows the scheme of such a potentiostat. Further they also require a very sensitive signal amplification circuit to make it possible to measure signals in the nano-ampere range. Care has to be taken to avoid very small measurement signals getting polluted by electronic noise.

Metal oxide sensors require only one function from their sensor electronics. They require their electronics to control their heating element. Depending on the kind of metal oxide sensor the heating of the sensor is done continuously or pulsed. Our best experiences are with continuous heating. This means the electronics must ensure a constant amount of power (Watt) is sent through the heating element of the sensor. Metal oxide sensors typically have a heating element with a relatively stable resistance. Because of this a constant voltage over the heating element does

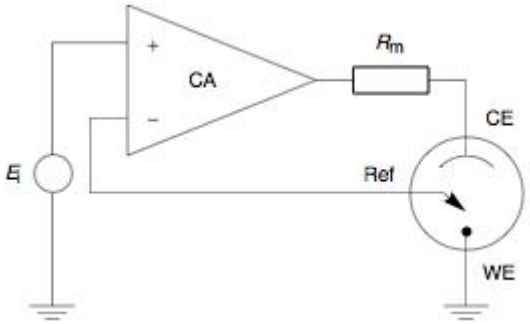

Figure 2.3: Electrochemical cell with potentiostat

ensure a sufficient stable power consumption in the heater element. For measurements over long periods (several weeks and longer) a possible change over time of the heater resistance has to be taken into account.

Power usage: Electrochemical sensors do not consume any power themselves. But, power is needed by the potentiostat and the signal amplification electronics. Metal oxide sensors always contain a heater element to bring the sensor on temperature. The typical power consumption of such a heater element is between 50 and 500 mW. Also, a small current need to be send through the sensing element to measure the sensor resistance.

Stabilization time: Both the electrochemical sensors and the metal oxide sensors have to be powered for a relative long period before they can be used. The potentiostat of an electrochemical sensor typically needs around 1 hour to stabilize the electrochemical cell. But, electrochemical sensors with a bias voltage different from 0 V may require a longer stabilization time. The Alphasense NO-B1 sensor for instance requires around one day to stabilize.

The metal oxide sensors can only be used after they have been heated up to the right temperature and after all impurities have had the time to be 'burned of' the sensor surface. Heating up the sensor goes relatively fast (less than one hour). How long it takes to burn the impurities from the sensor surface depends on how long it has been since the sensor has last been used. The needed 'cleaning time' can be up to one week.

We can here conclude it not possible to turn on an electrochemical or metal oxide sensor and start measuring immediately. A relative long waiting time is needed during which the sensor signal will stabilize. In practice, the easiest way to deal with this inconvenience is to keep the sensors powered at all times.

Sensitive to exposure to wind: Wind is one of the factors that influences the measurements of low cost gas sensors. Particularly metal oxide sensors are very sensitive to air being blown over them. This effect is caused by the cooling effect of the wind on the very hot sensor surface (e.g. 300 degrees Celsius). When designing the sensor housing, it is important to protect the metal oxide sensors against the wind while making sure the sensors are well exposed to the gas to measure.

Sensitive to direct exposure to the sun: Both electrochemical and metal oxide sensors should not be placed directly in the sun. Their measurement signal reacts strongly on exposure to the sun. With electrochemical sensors, direct exposure to the sun is known to dehydrate the membrane of the electrochemical cell.

Weather proof: Electrochemical sensors and metal oxide sensors have been used successfully outdoor during periods with a high humidity of the air. They have been tested during moments of rain, snow and fog. Both the sensors and their electronics continued their normal operations during those periods with high air humidity. During those tests, the sensors have always been covered by some kind of roof to avoid the rain could hit them directly. Also their electronics were kept powered at all times to have them slightly heated.

Temporal resolution: In the EveryAware project, we plan to conduct mobile air quality measurements. We expect to see a lot of variation in the sensor values during those measurements. The air quality sensors should be read out at a frequency of around 1 Hz to get a good view on this variation. Both metal oxide and electrochemical gas sensors can be read out at a high temporal resolution.

Sensitive to T and RH: Both, Electrochemical sensors and metal oxide sensors are sensitive to changes in relative humidity and temperature. The sensor housing should try to reduce the changes in T and RH to which the sensors are exposed. This could realized with the help of an air conditioning system. Such a system will be too expensive in the EveryAware context. Correcting sensor readings for changes in temperature and humidity will be a major issue.

Cross sensitivity: Low cost air quality sensors have issues with cross sensitivity. They do not only react on the gas they are supposed to measure but also on a wide variety of other gases. A lot of metal oxide sensors do for instance react on the presence of ozone. On some low cost gas sensors, filters and scrubbers are used to remove interfering gases before they reach the sensor surface.

2.3 Measurement of ambient air quality with low cost gas sensors: examples

The application of low cost sensors to measure ambient air quality is a continually developing field. Several studies and experimental projects have applied the use of low cost sensors to air quality measurements both on fixed and mobile platforms. The limitations of these sensors described in the previous section, makes their application quite challenging.

- The **Common Sense** project, primarily funded by Intel Labs Berkeley has developed a handheld device with a custom board that has carbon monoxide, ozone, NO_x, temperature, and humidity sensors (using the e2v MiCS 4514 and MiCS 2610 sensors and Citytech electrochemical sensors). In addition, they have developed a vehicular platform that is optimized for the particular challenges of municipal vehicles such as street sweepers [Aoki et al., 2009]. This system includes commodity mobile phones that connect to custom boards: one board has carbon monoxide, ozone, NO_x, temperature, and humidity sensors, while the other board contains the remaining electronics.

- The Institute for Software Integrated Systems (ISIS) at Vanderbilt University has developed the **Mobile Air Quality Monitoring Network (MAQUMON)**. The system consists of a number of car-mounted sensor nodes measuring different pollutants (O_3, CO and NO_2) in the air. The data points are tagged with location and time utilizing an on-board GPS. Periodically, the measurements are uploaded to a server, processed and then published on the SensorMap portal ([Institute for Software Integrated Systems], [Völgyesi et al., 2008]).

- **Sensaris** has fitted E2V sensors for O_3, CO and NO_x together with a GPS receiver, a noise sensor and Bluetooth communication into a portable sensor device the size of a wrist watch, called a Senspod. However, limited data is available in relation to the quality of the measurements themselves. Our own measurements with a Senspod next to a reference station showed low correlations for both CO and NO_x measurements.

- Within the **MESSAGE** project [Polak and Hoose, 2009], Alphasense electrochemical sensors have been employed with temperature and humidity compensations for CO, NO_2 and noise. These are both fixed and mobile in nature. The MESSAGE project invested quite some effort in the development of sensitive, low noise sensor electronics. Again, limited data is available relating to the quality of measurements obtained.

- The **Air Quality Egg** ([KickStarter, a], [The Air Quality Egg]) is an operational kickstart.com project, founded by Cosm (formerly called Pachube) which tries to realize a community-led air quality sensing network. The project has a low cost measurement device available for purchase, called the Air Quality Egg which suggest to be able to measure NO_2, CO, O_3, VOC's, radiation, and particulates. This project has been very successful in forming a community to supports its project financing and to discuss the products present and future features. The project uses an interesting approach by assuming it will once be able to interpret the data generated by the large amount of uncalibrated, and unvalidated measurement equipment they are rolling out at the moment.

- The **Sensordrone** [KickStarter, b] is a low cost keychain size measurement device able to measure reducing gases, oxidizing gases and other mixtures of gases (CO, H_2S, Alcohol, Hydrogen, and others) among a number of other components. Also this project was very successful in selling a lot of devices through kickstarter.com to a quite large community. Very interesting about this project is the development of a large amount of custom smartphone applications for the sensordrone, making it an easy to use and very multifunctional device.

What most of the above-mentioned projects have in common is that they are basically focusing on ICT and systems integration (with research teams mainly composed of ICT and electronics experts), and that very few tests have been carried out on the performance of the sensors themselves. This is not true for the MESSAGE project, but also here, nothing has been published about the measurement results.

2.4 Evaluation and selection of low cost gas sensors

Lab performance tests were carried out with several low cost gas sensors. The most promising ones were further tested in field conditions and compared to reference measurements. Also mobile and semi-mobile experiments have been conducted with the gas sensors. In this section an overview is presented of the most important results obtained. The focus is on NO_2, NO and CO gas sensors, since those are the best indicators of traffic pollution (see section 1.2.1).

2.4.1 Description of sensor tests

Lab tests were carried out with:

- Alphasense electrochemical sensors for CO (CO-BF), NO_2 (NO2-B1) and NO (NO-B1).

- Citicell electrochemical sensor NO_2

- E2V metaloxide sensors for CO (MiCS-5525) and NO_2 (MiCS-4514)

Three factory calibrated Alphasense CO sensors were respanned to a range of 0 - 10 ppm suitable for our purposes. The Alphasense NO_2 and NO sensors were tested both with standard electronics as purchased and with a Custom Sensor Solution Model 1402 Static Potentiostat [Custom Sensor Solutions] that was developed for the specific purpose of testing electrochemical sensors, because it was expected that the standard sensors' noise levels would be too high for use in ppb-range. Based upon the results of the lab tests field tests were carried out with Alphasense CO sensors, E2V CO and NO_2 sensors.

For all laboratory tests, synthetic gas mixtures were produced in a gas generation and distribution system. Temperature in the gas line was controlled at 25 degrees Celsius. The humidity was also controlled at an absolute moisture content of 1,15%, equating to a relative humidity of 50% at 20 degrees Celsius. An integrated multi gas measurement platform (Airpointer, Recordum Austria, www.recordum.com) was used as a reference monitor to verify the concentrations in the line. The instrument used in this study comprises a NO/NO_2 analyzer based on chemiluminescence (according to EN 14211) and a CO analyzer based on non-dispersive Infrared (NDIR) (according to EN 14626). For CO and NO a two stage dilution process was conducted to obtain the concentrations desired, and NO_2 was generated from the reaction between NO and O_3. The chamber used for testing the sensors was constructed of Teflon and connected directly to the gas line.

The non mobile field measurement was carried out in Antwerp during a 2 month period (30/11/2010 till 02/02/2011). The VMM (Vlaamse MilieuMaatschappij) station on the Plantin en Moretuslei in Antwerp was used as measurement location. The sensors were placed next to the VMM stations, around 30 meters from a street with much traffic. E2V CO, E2V NO_2 and Alpasense CO-BF sensors have been installed.

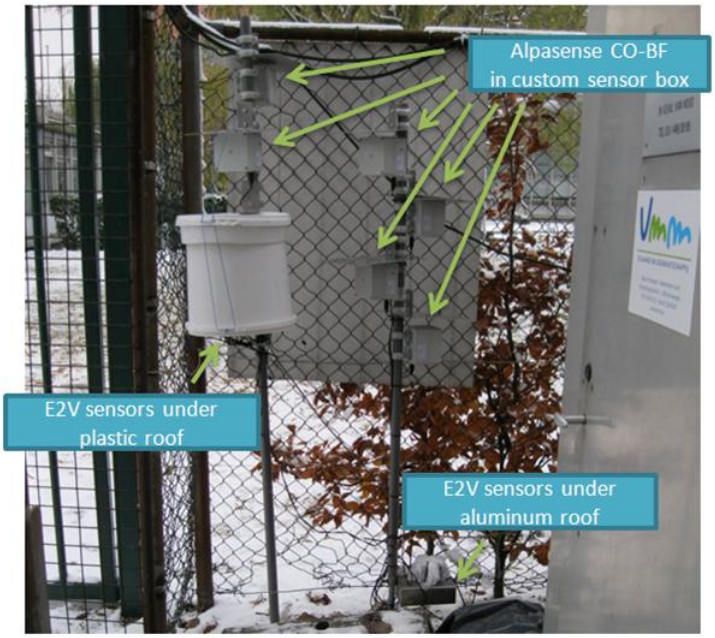

Figure 2.4: 6 Alphasense CO-BF sensors and 2 E2V CO and NO_2 sensors installed on VMM station Plantin En Moretuslei, Antwerp

2.4.2 Results with CO sensors

During lab tests the Alphasense CO-BF sensor showed acceptable reproducibility and linear response in the 0 - 10 ppm range (Figure 2.5).

The E2V CO sensors showed good reproducibility and stable signals in lab conditions (Figure 2.6).

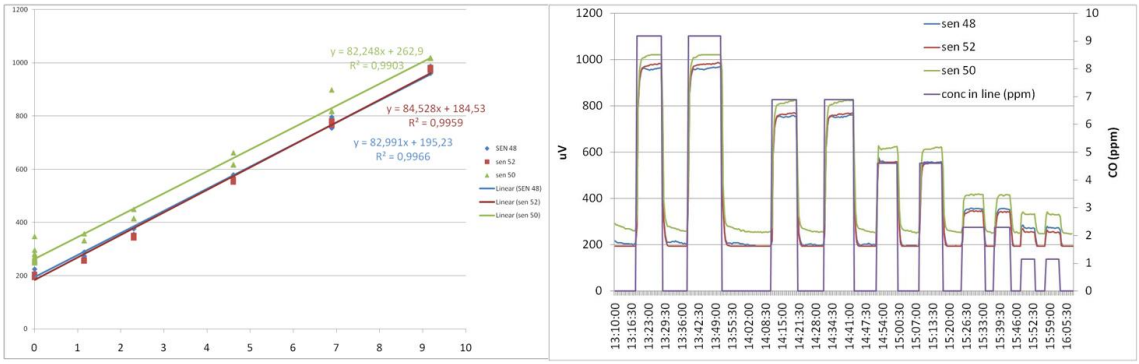

Figure 2.5: Results of laboratory tests with 3 Alphasense CO-BF sensors

They took about 3 minutes to reach their maximum signal. The sensor response is not that well linear in the 0-10 ppm range (Figure 2.7) and the R^2 values are around 95%.

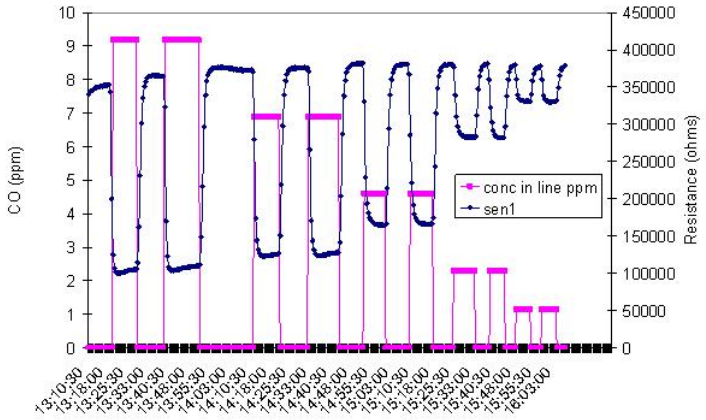

Figure 2.6: Results of laboratory tests with an E2V CO sensor

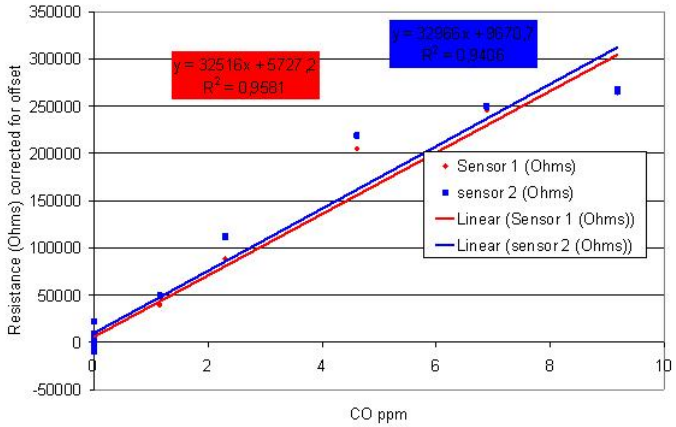

Figure 2.7: Response of 2 offset corrected E2V CO sensors in lab environment

The Alphasense CO-BF electrochemical cells are able to conduct reasonable CO measurements in outdoor conditions. In Figure 2.8 one of our best measurements with this sensor is presented. During a one month interval the CO-BF sensor follows the CO reference quite well. That this good measurement was obtained during the winter period was probably no coincidence. The measured

ambient CO concentrations are higher during the winter period. The CO-BF sensors turn out to be very sensitive to changes in temperature. In Figure 2.9 a more typical measurement result is presented from a CO-BF electrochemical cell installed at the side of the road during the spring season. We can distinguish the temperature effect on the sensor signal. We have observed this temperature effect on lots of CO-BF sensors during multiple measurement campaigns, it is quite typical for this sensor.

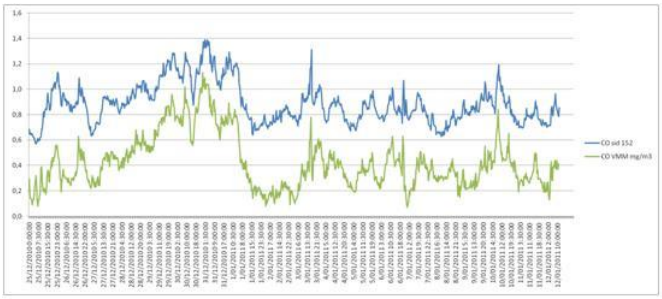

Figure 2.8: Alphasense CO-BF sensor next to VMM station Borgerhout during winter measurement

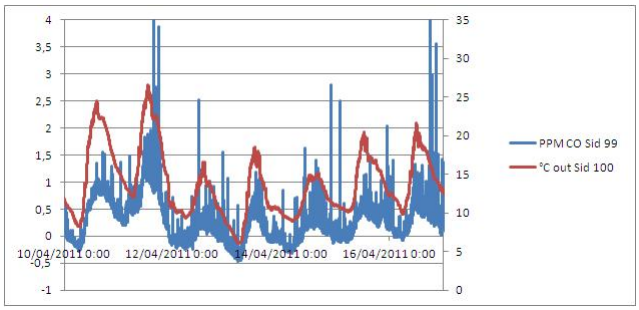

Figure 2.9: Alphasense CO-BF sensor installed in street Gent during spring period with temperature influence

Correcting the measurements of the CO-BF electrochemical cell for the influence of temperature is non trivial. Identical CO-BF sensors have a different temperature effect on their baseline signal. In Figure 2.10 13 identical CO-BF sensors have been installed next to each others in an office environment with no known CO sources in the close neighborhood. We see that some CO-BF sensors have a small temperature influence while others have a large temperature influence. Some sensors have a positive correlation with T, while others have a negative correlation. Furthermore, the sensor temperature influence may change over time with aging of the sensor and change of seasons.

The measurement results of the E2V CO sensors next to the VMM Borgerhout station differ significantly from the lab results. In Figure 2.11, we can clearly observe that the E2V CO sensors were unable to following the CO reference signal well. The obtained R^2 value was 14% for the E2V CO sensor under the plastic housing.

The measurements results of the E2V CO sensor can for a part be explained by the cross sensitivity of this sensor for the presence of ozone. In figure 2.12, the same E2V CO measurements are presented next to the ozone measurements of the VMM station. The obtained correlation of the E2V CO sensors turns out to be much better with ozone then with CO (R^2 = 72% for E2V CO sensor under the plastic housing).

In Figure 2.13 measurement results are presented from a different kind of measurement experiment. The AlphaSense CO-BF sensor was placed next to a black carbon (BC) sensor (microAeth Model AE51) on the back seat of a car during a drive through Brussels. Second measurements

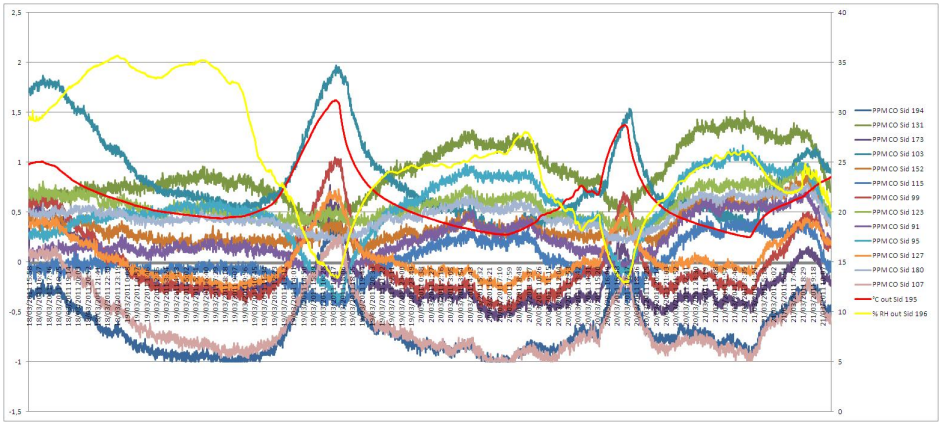

Figure 2.10: 13 identical CO-BF sensor installed next to each other in office environment with different temperature response

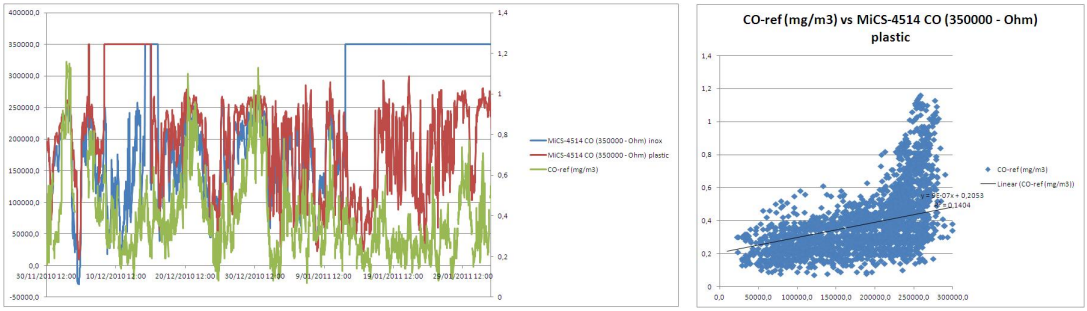

Figure 2.11: E2V CO sensors installed next to VMM Borgerhout station, against CO reference

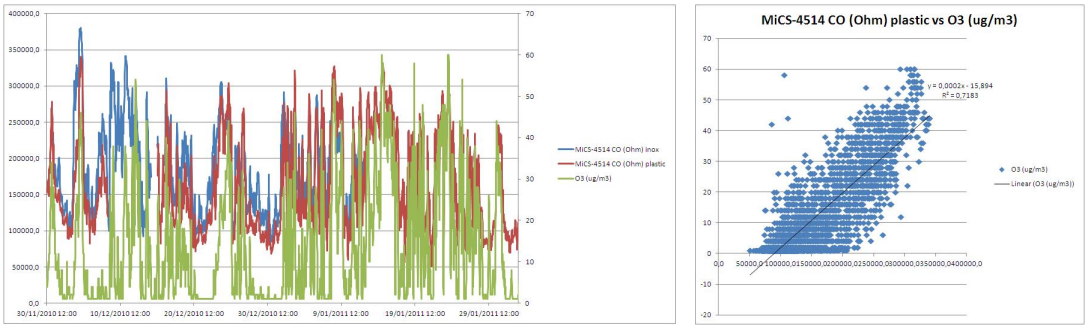

Figure 2.12: E2V CO sensors installed next to VMM Borgerhout station, against Ozone reference

were collected from both the CO-BF and BC sensor. 15 seconds gliding averages have been calculated of the BC measurements to reduce noise. Both measurements follow each other quite well. This indicates low cost CO measurements may have potential to be used for the identification of traffic pollution hotspots. The CO concentrations present were quite high during this mobile measurement.

In Figure 2.14 a scatter plot is drawn of the CO and Black Carbon (BC) measurements. There seems to be a very good linear relationship between between the two components. The CO and BC sensor raise at the same hotspot locations. The obtained correlation is quite high, R^2 = 82,5%. This indicates measurements of the CO-BF sensor may be well fitted for relative traffic pollution measurements.

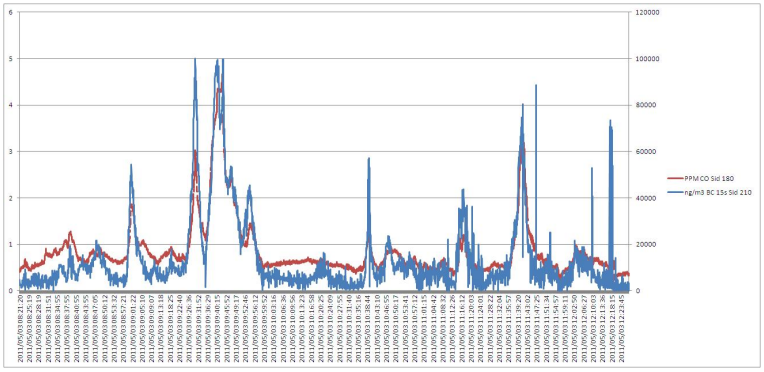

Figure 2.13: Alphasense CO-BF sensor placed next to MicroAethalometer on back seat of car during drive through Brussels

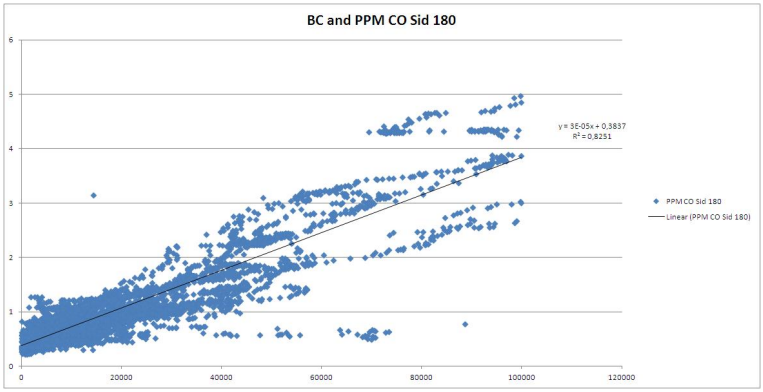

Figure 2.14: Scatter plot of Alphasense CO-BF sensor placed next to MicroAethalometer on back seat of car during drive through Brussels

2.4.3 Results with NO_2 and NO sensors

The E2V NO_2 metal oxide sensors were placed on an E2V sensor evaluation board and placed within the sample chamber. The per second resolution data was aggregated to 30 second averages.

The sensitivity of the sensor was good. Even low concentrations of 25ppb NO_2 were well detected. Response times were slow with maximum response achieved between 4 and 5 minutes. The response across the range of concentrations tested was observed to be linear with acceptable scatter (Figure 2.15).

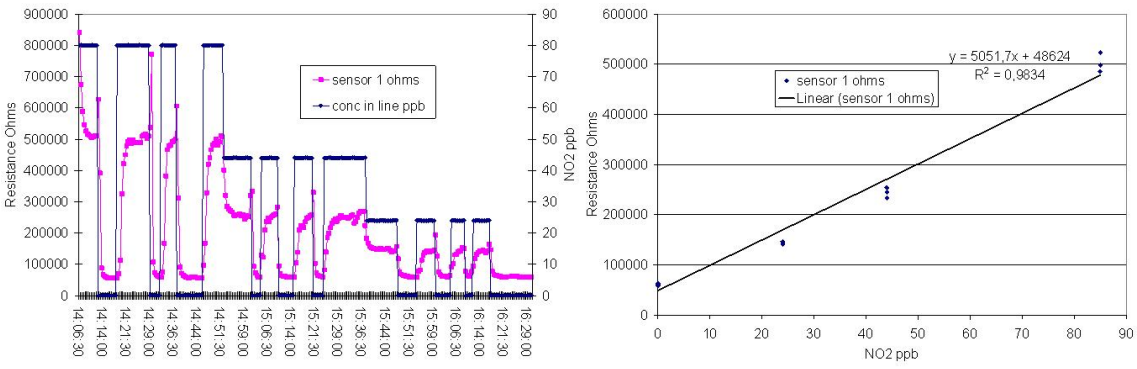

Figure 2.15: Results of laboratory tests for e2v NO_2 sensor

The noise on the Alphasense NO_2 and NO electrochemical sensors as supplied by the manufacturer was too high to do any useful measurement in the 0 - 200 ppb range. Even when fitted with the Custom Sensor Solutions electronics board, the high degree of noise makes it difficult to envisage these sensors being readily useful in ambient uncontrolled environments.

The Citicell NO_2 sensors showed a relatively large degree of noise. Full scale response was typically achieved within 5 minutes. Response was observed to be linear, however, reproducibility and variance of a constant signal were both relatively poor compared to the cheaper e2v sensors.

During the field measurements, the NO_2 measurements of the E2V NO_2 sensors in ambient air were very poor. In Figure 2.16 we can observe the E2V measurements don't follow the NO_2 reference measurements. The NO_2 sensor seems to have a negative response on the presence of NO_2, while in laboratory conditions the sensor responds positively to increasing NO_2-concentrations. Interference from the presence of ozone on the sensor signal can explain the obtained measurements results. The obtained correlation between the measurement signal and the ozone concentrations present was R^2=85% which is quite high (Figure 2.17).

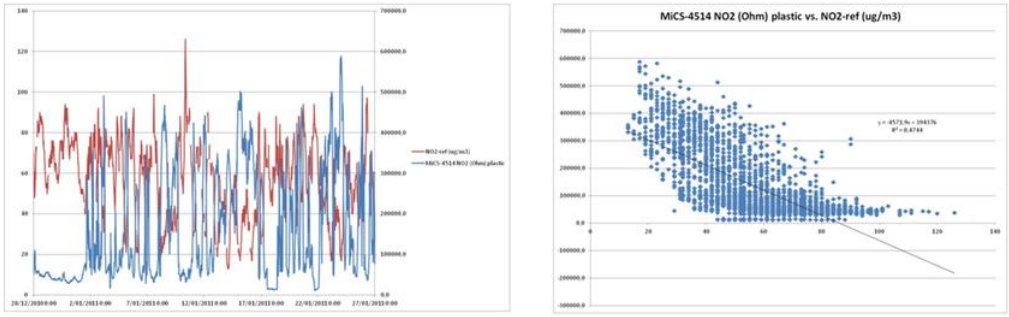

Figure 2.16: E2V NO_2 sensor placed next to VMM Borgerhout with NO_2 reference

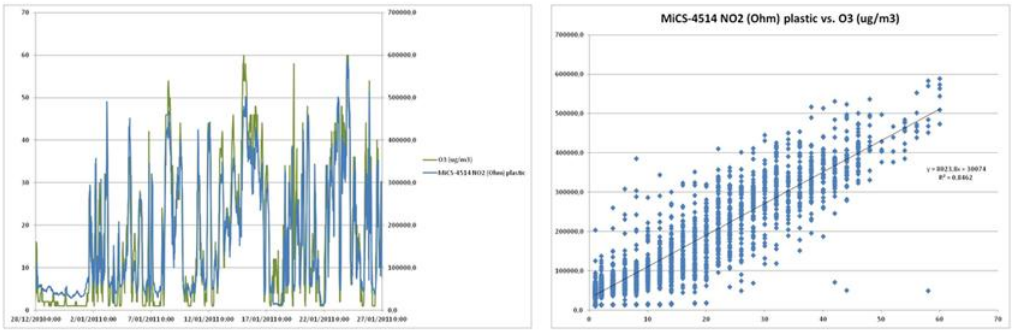

Figure 2.17: E2V NO_2 sensor placed next to VMM Borgerhout with O_3 reference

2.4.4 Conclusions and sensor selection

We can conclude individual low cost gas sensors are not fitted to measure low concentrations of CO, NO_2 and NO. Although the sensors do obtain good results when measuring CO and NO_2 concentrations in a controlled lab environment, those results could not be reproduced during outdoor measurements in ambient air next to a reference measurement station. The influence of disturbing factors such as meteorological factors and the presence of ozone is too large to distinguish small changes in the concentration of the gas to measure. On the other hand, individual low cost gas sensors can be used to conduct relative measurements. It has been observed the Alphasense CO-BF sensor follows quite well the black-carbon measurements during mobile measurement campaigns in urban environments where higher concentrations of traffic pollution are

present. This may indicate relative low cost CO measurements have potential to be used for relative traffic pollution measurements. Although this does not allow them to be used for absolute air quality measurement, they may allow us to identify locations with higher presence of traffic pollution during mobile measurements. The disadvantage of using electrochemical gas sensors for the EveryAware SensorBox is their relative high cost (180 Euro, electronics included). Realizing the same results with a collection of metal oxide sensors could reduce the hardware price significantly.

The observed low cost NO_2 measurements seem to have less potential then the low cost CO measurements. This can be explained by the lower concentrations of NO_2 present compared to the CO concentrations. Still, low cost NO_2 measurements are promising at locations where many diesel vehicles are present and higher NO_2 concentrations are expected.

The usability of individual low cost gas sensors for the measurement of ambient traffic pollution concentrations turns out to be quite limited. We try to deal with this issue by combining the air quality sensors in an sensor array. Since each sensor reacts differently on the changes in their environment, the sensor array algorithm may be able to make a distinction. The following sensors have been selected for the EveryAware SensorBox:

- **Alphasense CO-BF CO sensor:** Of all tested low cost gas sensors, this sensor obtained the best results for detecting the presence of traffic pollution. With it's price tag of around 180 euro (sensor electronics included) it is also by far the most expensive selected gas sensor. Although the electrochemical cell does not use any electricity itself, the used sensor electronics do require up to 200 mW.

- **E2V MiCS-5521 CO sensor and MiCS-2710 NO_2 sensor:** The sensors are not well suited to be used as stand-alone air quality sensors due to quite large problems with cross sensitivities. We believe they have potential when being combined with other sensors in an sensor array. The sensors have proven to be able to react on low CO and NO_2 concentrations present in ambient air. With a price tag of less then 5 euro a piece, they are very attractively priced. Thanks to their micro-hotplate technology, their power usage stays quite low (less then 100 mW).

- **E2V MiCS-5525 CO sensor with charcoal filter:** This sensor contains exactly the same sensitive element as the MiCS-5521 CO sensor. This sensor only differs by the presence of a charcoal filter which has been added on top of the sensitive element. Although we noticed this charcoal filter to increase the sensor reaction time and reduce the sensor sensitivity, it also enhances the selectivity of the sensor. With a price tag of less then 5 euro, we believe it may be able to offer us a cost effective way to help distinguish the target gas from interfering gases.

- **Figaro 2201 gasoline and diesel sensor:** This is a metal oxide sensor which contains two sensing elements. One which is specially designed to react on the presence of gasoline exhaust fumes (mainly on CO, H_2 and HC) and a second to react on the presence of diesel exhaust fumes (mainly on NO_x). Figaro designed this dual sensor for the automotive industry to be used in intelligent vehicle ventilation systems. Although this sensor was not included in the lab experiments, we observed this sensor to react on the presence of traffic pollutants in ambient air. Just as the E2V sensor, also this metal oxide sensor seems be quite sensitive to cross sensitivities, making it a requirement to combine this sensor with other sensor to realize reliable air quality measurements. With a price tag of around 15 euro and a power usage of around 500 mW, the Figaro has slightly less attractive specifications.

- **E2V MiCS-2610 Ozone sensor:** The selected E2V sensors have proven to be very sensitive towards the presence of ozone during the field experiments. For this reason, we expect an Ozone sensor may be able to add additional useful information to the sensor array. Also this E2V sensor has a low power usage and price tag.

- **Applied Sensors AS-MLV VOC sensor:** With this sensor, Applied Sensors is on the first place aiming on automated ventilation systems which need to be able to detect a bad indoor air quality. The concentrations of VOC in an indoor environment can be significantly higher as in an outdoor environment. Since traffic pollution also contains VOC, this sensor may be able to add information to our sensor array.
- **Sensirion SHT21 T and RH sensor:** Low cost gas sensors are very sensitive to changes in both temperature and relative humidity. By adding high quality temperature and humidity sensor to the sensor array we expect to be able to enhance the obtained measurement results. The combined sensor of Sensirion was selected due to its high measurement precision and our good experiences in the past with these sensors.

In table 2.1 an overview is presented of the key properties of the selected low cost gas sensors. All sensor specifications from this table are taken from official sensor data sheets.

Table 2.1: Key properties of selected low cost gas sensors

Sensor name	Component to measure	Power usage	Meas. range	Indicative price
Alpasense CO-BF	CO	0 mW	0-5000 PPM	180 Euro*
MiCS-5521	CO	76 mW	1-1000 PPM	3,4 Euro
MiCS-2710	NO_2	50 mW	0.05-1 PPM	3,7 Euro
MiCS-5525	CO	76 mW	1-1000 PPM	5 Euro
Figaro 2201	Gasoline exh. (CO, H2, HC)	500 mW	10-1000 PPM	15 Euro
”	Diesel exh. (NO_x)	500 mw**	0.1-10 PPM	”
MiCS-2610	O_3	95 mW	10-1000 PPB	3,7 Euro
AS-MLV	VOC	41 mW	NA	15 euro

* 60 Euro for sensor and 120 Euro for sensor electronics
** This is the same heater as for the gasoline sensor. The total usage of the dual Figaro sensor is 500 mW.

Chapter 3

SensorBox proposed design and implementation

The SensorBox is a portable device which will allow people to measure the air quality around them during everyday life. To accomplish this task it has to be cheap, small, light and low power as much as possible, but allowing to perform reliable measurements. For this reasons the SensorBox is composed by two main parts: a **SensorBoard** containing all gas sensors, and a **ControlBoard** where all the other electronics devices are integrated (e.g. signal conditioning, GPS, communication ports). The main issues about the SensorBoard concerns the signal conditioning to avoid noise problems and the gas chamber design to reduce external disturbances on the measurements, as will be discussed in the next sections.

3.1 SensorBox requirements

In this section, we describe all requirements imposed on the EveryAware SensorBox. First, the requirements imposed by the sensors on their electronics are discussed. Second, as described in chapter 2, we want to combine the measurement signals of the 10 sensors present in the EveryAware SensorBox in an sensor array. To make this possible, it is crucial all 10 sensors in the SensorBox are exposed to the same, homogeneous gas mixture. This homogeneous gas mixture is realized with the help of a sensor chamber of which the requirements are described in the second section. Third, the user requirements for the SensorBox are discussed.

3.1.1 Requirements for sensor electronics

High sensitivity electronics

The low cost gas sensors should be able to react on the small changes in gas concentrations, present in ambient air. For CO they should be able to detect changes of 0.1 ppm, and for NO_2 changes of 10 ppb. Note that this are small changes compared to the measurement ranges the used sensors are intended for by their manufacturers (Table 2.1). For this reason, quite sensitive sensor electronics are required.

Wide measurement range

Low cost metal oxide sensors of the same model, even of the same production date, have a significantly different sensor baseline and response. Because of this each sensor needs to be calibrated separately. Another consequence of this is that the sensor electronics must be able to

deal with the (large!) differences in sensor baseline and sensor response. The sensor electronics has to support a wide enough measurement range to support the variability between MOX sensors.

Low noise sensor electronics

It is important to avoid electronic noise on the sensor signals to be able to distinguish the small reactions of the sensor signals. This can be accomplished by minimizing the amount of electronic noise being picked up by the sensor electronics and by removing picked up electronic noise with for instance digital and analogue low-pas filters.

Sensor heater voltages

Metal oxide gas sensors contain a sensitive element that has to be kept at a quite high temperature (300 - 400 degrees Celsius) to be able to operate. It is crucial for the correct operation of the sensor that the correct power is applied to the sensor heater element to keep the sensor element at the right temperature. Even relative small changes in the applied heater power can reduce both sensor sensitivity, selectivity and response time. Which heater power needs to be applied is strongly sensor dependant. In Table 3.1 an overview is given of the voltages which need to be applied to the heater element of each selected metal oxide sensor.

Table 3.1: Heater voltages of selected metal oxide sensors

Sensor name	Sensor heater voltage
MiCS-5521	2,4 V
MiCS-2710	1,7 V
MiCS-5525	2,4 V
Figaro 2201	5 V
MiCS-2610	2,35 V
AS-MLV	2,7 V

3.1.2 Requirements for sensor chamber

Protection against meteorological factors

Low cost gas sensor measurements are heavily influenced by a number of meteorological factors: temperature, humidity, and exposure to wind and sun. The sensor chamber of the EveryAware SensorBox has to play a mitigating role on the exposure of the low cost gas sensors to those meteorological factors.

Air flow and placement of sensors inside sensor chamber

The way the air flow is sent through the sensor chamber has a big influence on the obtained sensor measurements. For the sensor array algorithm, all sensors need to be exposed, as much as possible, to the same homogeneous gas mixture. Mixing of the gas can be enhanced by applying techniques such as letting the gas enter the sensor chamber under a corner.

Although, placing the sensors in a row between the gas inlet and outlet may seem like a logical choice, it is not the best way to expose all sensors to the same gas mixture. The gas does not move in a linear way over the sensors between the gas inlet and outlet due to turbulence in the gas flow when the air enters the sensor chamber. The most homogeneous gas mixture is expected to be found away from the gas entrance. Instead of putting all sensors in a row, we can expect better

result by moving them all to the back of the sensor chamber, away from the gas inlet. Furthermore it is favorable to place the most robust sensors with stable sensor signals closest to the gas inlet since we expect their sensor signal to be less influenced by fast changes in the gas mixture. The Alphasense CO-BF electrochemical cell meets this requirement well. The 'robustness' of this sensor may be caused by the fact all gasses have to diffuse first through the membrane of this sensor.

The Figaro TGS 2201 sensor produces quite some heat due to it's relatively large power usage of 0,5 W. To limit the heating up of the sensor chamber by this sensor it should be placed close to the gas outlet. Furthermore it is important the temperature measurements should not be done too close too this sensor. Close to the gas outlet of the sensor chamber, we can expect the presence of some more wind. Since this will be a very constant air flow which is not that big, we don't expect it to have a negative influence on the used gas sensors.

The corners of the sensor chamber are typically less well ventilated. For this reason it is better to avoid placing sensors directly in the sensor chambers corners.

The disadvantage of reserving some space in the sensor chamber for gas mixing is that it may increase the size of the sensor chamber. The requirement for additional space can be minimized by using the gas mixing space on the PCB for electronics such as cable connectors, resistors and potentiostats. We are well aware a pragmatic approach may be needed. In Figure 3.1 an 'optimal' sensor placement in the sensor chamber is proposed. The actual sensor chamber has to be larger due to space requirements of the needed sensor electronics. By placing the sensor electronics in an optimal way (in the mixing space) it may be possible to come close to this optimal sensor placement.

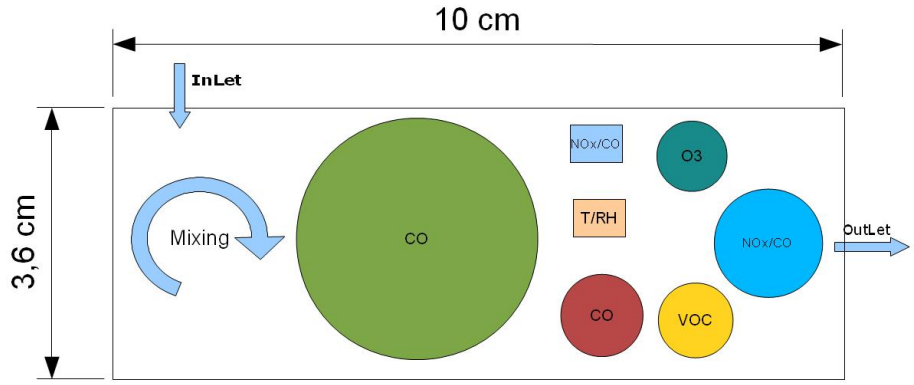

Figure 3.1: 'Optimal' sensor placement in sensor chamber

Optimal flow speed through sensor chamber

The air flow speed through the sensor chamber is expected to have a significant impact on the measurements of the metal oxide sensors. Higher air speeds give a faster refreshment of the gas mixture inside the sensor chamber. This allows faster response times on air quality changes while it makes the environment of the sensors less stable. This may cause lower quality measurements. Further, higher air speeds will cool the metal oxide sensors down (wind effect). This influences both the sensor sensitivity, selectivity and response time. Also, higher air speeds may avoid heating up of the sensor chamber due to the metal oxide sensor heater elements and sensor electronics.

The selected refreshment rate will always be a weighted compromise of the factors mentioned in the previous paragraph. For the EveryAware SensorBox, we opt for a gas flow high enough to refresh all gas in the sensor chamber within only a few seconds. Because we expect better results from the sensor array algorithm when all sensors are faster exposed to changes in the measurement environment.

Usage of pump or fan

The EveryAware SensorBox requires the usage of a pump or fan to establish a continuous air flow through the sensor chamber. In the past, we obtained quite good results with the SP 550 EC Eccentric diaphragm micro pump of Schwarzer Precision to generate a continuous gas flow over metal oxide air quality sensors. Although this pump is well fitted for the construction of air quality measurement devices, it is not necessarily the best choice for the EveryAware SensorBox. In Table 3.2, the key properties of the SP 550 EC pump are placed next to the specifications of some low cost mini fans: the Micronel F17LM-9 fan, and the COPAL F17HA-05 MC fan.

Table 3.2: Key properties of Schwarzer Precision SP 100 EC eccentric diaphragm micro pump, Micronel F17LM-9 fan, and COPAL F17HA-05 MC fan according to their datasheets

SP 550 EC pump	F17LM-9 fan	F17HA-05 MC fan	
Manufacturer	Schwarzer Precision	Micronel	COPAL
Free flow	1,8 liter/minute	15 liter/minute	15 liter/minute
Power usage	0,45 W (max)	0,2 W	0,15 W
Dimensions	41 x 23 x 34 mm	17 x 17 x 8 mm	17 x 17 x 8 mm
Noise	N/A (quite loud!)	7 dB(A)	7 dB(A)
Price	110 Euro	10,78 Euro	NA
Voltage	4,5 V	5 V	5 V
Weight	41 gr	2,3 gr	2,3 g

The key properties from the Micronel F17LM and COPAL F17HA-05 MC datasheets presented in Table 3.2 are promising compared to the ones from the SP 550 EC pump. The fans are cheaper, smaller, lighter, and quieter. Also they have a lower power usage and a higher free flow then the pump. For this reason, the usage of a low cost fan in the sensor chamber of the EveryAware SensorBox is evaluated in 6.1.1.

Fans are a lot more sensitive to pressure differences inside and outside the sensor chamber then pumps. In Figure 3.2, a graph is shown of the flow reduction through the F17LM-9 mini-fan when a pressure difference is applied between both sides of the fan. We can observe the flow through the fan is reduced to 0 when a static counter pressure of 10 Pascal is present. Since 10 Pascal is a rather low pressure ($1bar = 10^5 Pa$), care needs to be taken in the design of the sensor chamber to avoid the build up of a pressure difference over the fan. The gas flow should be able to travel freely through the sensor chamber with a minimal amount of obstacles.

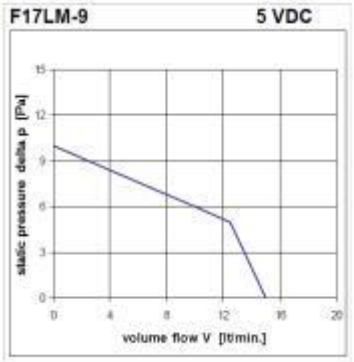

Figure 3.2: Flow in lt/min of F17LM-9 5V fan when counter pressure is present (source: F17LM-9 data sheet)

Air tightness of sensor chamber

From the theoretical point of view, all gas should enter the sensor chamber through the gas inlet and leave the sensor chamber through the gas outlet. The sensor chamber should be perfectly air tight with no gas leaving or entering the sensor chamber through small, unintended cracks. All electronic cables entering the sensor chamber should do so in an airtight way and the lit of the sensor chamber must be airtight.

We know from experience, realizing a guaranteed air tight sensor chamber is not an easy thing to do. To avoid that small cracks in the sensor chamber could cause gas to enter unintended in the sensor chamber, we have to keep the sensor chamber on a small overpressure. This way, gas will only leave the sensor chamber through the small cracks, but will not enter. The small overpressure in the sensor chamber can be realized by placing the pump or fan at the gas inlet of the sensor chamber, instead of placing it on the gas outlet.

3.1.3 User requirements

Usability

The EveryAware SensorBox is intended to be used by Citizen Scientist. For this user group, a device which is very easy to use, without the requirement of a user manual is preferred. To realize this, the amount of buttons on the device should be limited to the absolute minimum. Ideal would be a device with only a single button, the power button.

Price

The EveryAware SensorBox needs to be low cost. A bill of material of only a few hundred euro is desirable.

Easy to handle

The EveryAware SensorBox should be easy to carry around. It should hinder the user as little as possible during his everyday movements. This required the SensorBox to be limited in size and weight, to be quite, and to have a large autonomy. Furthermore, we know from previous experiences with volunteers they like measurement devices to be 'discrete'. Volunteers want to be able to conduct measurements without drawing too much attention from their environment. As a way to meet both requirements we want the EveryAware SensorBox to be fitted for usage from within a back-pack, purse, or other bag. To allow this, following additions are needed to the EveryAware SensorBox: First, the air has to enter the sensor chamber through a tube. This way, only a subtle tube will be visible from outside the back-pack. An example of a gas tube used for this purpose is shown in Figure 3.3 (left side). Second, care has to be taken that the gas outlet of the SensorBox can not easily get blocked when the EveryAware SensorBox is placed within a back-pack containing other items. In Figure 3.3 (right side) the gas outlet protection designed for the first EveryAware SensorBox prototype is depicted.

3.2 Electronics design

The architecture of the SensorBox is based on Arduino [Arduino open-source electronic prototyping platform], an open-source electronics prototyping platform based on flexible, easy-to-use hardware and software. The micro-controller on the board can be easily programmed to accomplish the tasks of the project. This system was chosen because of the simplicity with which is

Figure 3.3: Gas inlet tube placed in front of fan (left) and gas outlet protection (right)

possible to connect different component (shields) like GPS, Bluetooth or many others. Indeed, different shields are available on the market: they are ready to be connected and often there is a library to start programming. Considering that there is no need for complex data elaborations and that power consumption is an issue, Arduino is a good choice to have a prototype in short time. Furthermore, being an open-source project it is be possible, as we did, to review all the schematic and make a custom board with reduced dimension and cost, improving some parts if needed.

The development of the SensorBox followed various steps: after having tested each single device with the Arduino board, a first version (in the followings called *Version 1* or SB1) of the SensorBox has been produced in order to test the integration of the whole system and start testing. Then, a second version (in the followings called *Version 2* or SB2) has been designed with improvements on cost, weight, dimensions and signal integrity. The main step that has been achieved in *Version 2* is the implementation of a new electronic design based on a 4 layers Printed Circuit Board (PCB).

In the next sections a brief description of these system is reported.

3.2.1 SensorBox Version 1

The first version of the SensorBox is composed by two main parts, like shown in Fig. 3.4: a SensorBoard and a ControlBoard. In addition to them a battery to power the electronics and an air pump (or fan) are required to generate a constant air flow in the sensor chamber.

The **SensorBoard** is composed by all the gas sensors and the temperature/humidity sensor. There are also mechanical trimmers needed to regulate the output of each sensor for calibration. This board is positioned inside an isolated chamber to allow as much as possible a constant air flow over the sensors, limiting wind, sun and temperature influence on the measurements. Initially, an air pump has been used to push the air inside the chamber. Later, it has been substituted with a cheaper fan. Even if the air pump allows better performance, the fan permits acceptable results with a considerable saving of money.

The **ControlBoard** is composed by two parts: an **Arduino Mega 2560** microcontroller system and a **ShieldBoard**, a custom-build PCB with all the additional components required by the SensorBox:

- a GPS shield, used to localize the measurements;
- an SD card shield, used to locally store the data when the measurements are not delivered in real-time to the smartphone;
- a Bluetooth shield, used to communicate with the smartphone and send the measurements;

At the startup, the firmware on the microcontroller waits for the GPS to acquire the coordinates (one for each second). Next, it reads from the ADC the outputs of the gas sensors and stores the data on the SD card. When a Smartphone activates a Bluetooth connection, it is possible to read the measurements directly from the phone in real-time. The whole system is powered by a

lithium battery of 4000 mAh, rechargeable through a USB connection. This capacity allows the SensorBox to work for 6 hours.
This version of the SensorBox mainly brought up the following problems:

- weight and dimensions were quite large, still allowing to carry it inside a backpack;
- the sensor chamber was not perfectly isolated from the other parts of the box;
- signal noise caused misreadings from sensor values.

All these problems have been resolved in the design of *Version 2*.

Figure 3.4: *Version 1* of the SensorBox packed in a plastic box with holes and pipes for the air flow regulation

3.2.2 SensorBox Version 2

The second version of the SensorBox tried to solve all the previous issues. As it is possible to see in Fig. 3.5, the system has been integrated reducing weight and dimension.
The **SensorBoard** design implements the sensor positioning that brings a smaller board with an optimal air flow over the sensors. A small fan is used to push the air inside the sensor chamber. The actual implementation of the sensor chamber together with the overall box enclosure is still under evaluation, and different solutions (commercial boxes and custom ones) are being considered. Output signals can always be regulated by the trimmers and an LC filter has been inserted for each sensor in order to reduce high frequency noise.
The **ControlBoard** has been integrated in a single PCB including the Arduino Mega 2560 design with the other devices, such as Bluetooth, GPS and micro SD card. These components are different from the ones used in *Version 1* because they have been found as smaller, requiring less power and with improved signal strength. A 5 V voltage regulator has been added to avoid voltage drop from the battery and stabilize supply voltage. This implies also a better gas sensor output signal. The firmware on the microcontroller is an improvement of the previous version, doing an oversampling and filtering of the sensor output (10 times per second). This way it is possible to reduce the high frequency noise further.

the SensorBox is powered by an external USB battery because it allows to be more flexible on the choice if a larger battery (capacity, weight and dimension) is preferred over a smaller one or vice-versa, according to the specific use case.

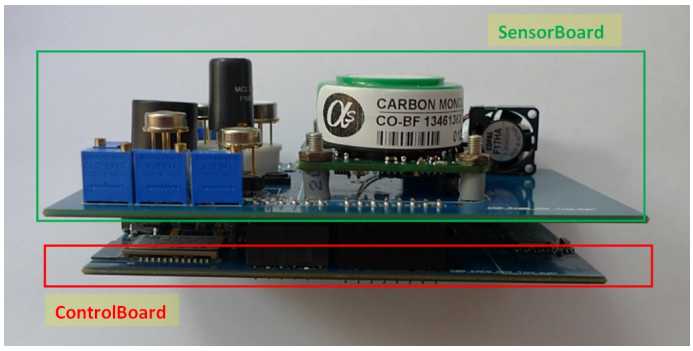

Figure 3.5: *Version 2* of the SensorBox implemented with custom PCBs (4 layers for ControlBoard and 2 layers for SensorBoard)

Chapter 4

Evaluation of the noise pollution with smartphone's sensors

4.1 Introduction

The potential of using mobile devices to measure sound has only been realised relatively recently and the scientific aspects of measuring noise using mobile phones is very much under-researched. This issue is compounded by the relative ease with which developers can build sound measurement Apps, permitting their deployment by teams who may not have an in-depth scientific understanding of sound or access to appropriate calibration tools.

The App under evaluation [Everyaware Project, 2012] was developed by a third party [Widetag, 2012] and pre-dated the EveryAware project. Thus, the evaluation process sought to understand the behaviour of the App and hosting device as an assemblage. Two main aims for evaluation were identified. Firstly, it is important to develop an understanding of the technical characteristics of the WideNoise Application and mobile devices on which it is deployed, to enable the level of accuracy to be taken into account for the interpolation of the resulting data (more details about the interpolation process are given in Section 4.2).

The second, equally important, objective was to be able to identify a clear and coherent language for communicating the level of accuracy to the users participating in noise-related campaigns or otherwise using the App. These two goals framed a number of the decisions made in terms of the approach taken to technical evaluation.

This section of the report presents an overview of the evaluation process used, which encompassed both device calibration and software evaluation. This is followed by a summary of the results obtained, and considerations as to their implications for the EveryAware project as a whole.

4.2 Background - Device Calibration

The general approach taken to any calibration process is to compare the results obtained on the device in question with those of a higher quality (pre-calibrated) device. This will permit a greater understanding of how the device behaves under various conditions of use.

In the case of sound, such calibration should ideally be undertaken within an anechoic sound chamber (an anechoic chamber is a room in which the walls, ceiling and floor are lined with a sound absorbent material to minimise reflection, and also permits the identification of sound at much lower thresholds than a normal environment due to soundproofing [UCL, a]). Comparative measurements are made using a reference Class 1 meter (which is a Precision Grade for laboratory and field use with an error of $\pm$ 0.7 dB [Noise Meters Limited] and is designed to meet standards defined by the International Electrotechnical Committee [Cirrus Research plc UK].

Sound is generally measured in deciBels (dB) and *A-weighted* sound pressure level – expressed in dB(A) – is the defacto way to measure (urban) noise, as prescribed by [European Parliament and Council, 2002, Annex 1] and [International Organization for Standardization, 2007]. Further details can be found in the project deliverable D4.1. White noise is considered to be the most suitable sound source for these tests, since calibrating against single tones is not sufficiently accurate [Santini et al., 2009; Stevens, 2012]. White noise contains a uniform distribution of sound frequencies without any bias for any particular frequency. While using a recording of particular target sounds could be considered, white noise also permits a better understanding of the behaviour of a device under real world conditions.

Prior research has shown that the discrepancy between mobile phone and the trusted device is not constant across the sound level range and the discrepancy is often not linear [Stevens, 2012, pp. 204-206]. As it is important to understand the behaviour of a device over a full range of sound, for calibration purposes fixed levels of A-weighted sound are generated within the sound chamber and measured simultaneously both by the Class 1 meter and by the device under test. Intervals of 10 dB(A) steps are chosen, since each increment is perceived to be twice as loud by the human ear and this allows a simple communication of the results to non-technical users.

Importantly, different devices respond differently depending on the inbuilt microphone [Stevens, 2012] and where possible a range of devices should be tested. Once behaviour at the fixed 10 dB(A) intervals is identified - i.e. the key nonlinear discrepancies noted - these can be used as input to an interpolation process to model the behaviour of each device across a range of sound between the fixed intervals [Stevens, 2012]. This interpolation process forms part of a software-based calibration process which takes the raw values output from the microphone and converts them to dB(A).

4.3 Methodology

The evaluation described here is based on work carried out by previous researchers including [Maisonneuve et al., 2010; Santini et al., 2009; Stevens, 2012]. To understand the behaviour of a sound measuring device, it is important to understand both its response to the fixed-point measurement process described above (the 10 db(A) intervals), as well as how the conversion between the raw microphone reading and output is carried out within the software, including any interpolation. Both of these issues were investigated as part of the WideNoise test as in the case of WideNoise the displayed sound level measurement couples both the device's response to the sound and any subsequent software processing and it was not possible to decouple them at the time of testing (although the source code was subsequently made available to the EveryAware team).

4.3.1 Testing Responses to Fixed Sound Levels

The evaluation took place in the sound chamber at the UCL Ear Institute [UCL, b] which is an anechoic sound chamber as described above. The WideNoise App was installed on six different phones (iOS and Android) to be able to evaluate behaviour across the different platforms and different models, and a Class 2 sound meter also introduced alongside the Class 1 reference meter. The phones were mounted on a pedestal which also held the reference meter. The reference meter was calibrated before the experiment by the assistant using a sleeve calibrator.

Using a laptop white noise was played through a speaker system into the sound chamber starting with 100 dB(A) going down to 90, 80, 70, 60, 50, 40 and finally 31.

These sound levels were set via the reference device and the corresponding WideNoise reading taken from each of the mobile phones. This sequence was repeated at least twice at each decibel step to confirm the measurements obtained. Within the environment of the sound chamber the

Table 4.1: Results Obtained from the Calibration Process

Class 1 Reference Meter	31 dB(A)	40 dB(A)	50 dB(A)	60 dB(A)	70 dB(A)	80 dB(A)	90 dB(A)	100 dB(A)
Class 2 Sound Meter	35.5	41.8	50.5	60	70	80	90	100
iPod Touch	50	56	64	74	83	93	90	96
IPhone 4	19	35	57	67	80	90	94	96
IPhone 3	42	34	51	64	73	85	93	107
HTC	57	57	60	66	73	88	93	99
HTC Explorer	24	51	61	65	74	89	93	99
Huawei Blaze	51	52	54	57	64	74	84	94

quietest testing level achievable was 31dB(A) this was likely due to the fact that the door had to be left ajar for testing to occur.

Importantly, it was decided to calibrate against dB(A) (even though WideNoise application does not apply any weighting) to be able to offer a comparative data type for the project participants. It was assumed that the participants would be expecting dB(A) a to be able to have a number they could compare to the official regulations for urban noise which are based on dB(A) [European Parliament and Council, 2002, Annex 1].

4.3.2 Analysis of the WideNoise Sourcecode

The second component of the analysis involved the investigation of the WideNoise source code, which was made available to the EveryAware team as part of the project. The review was carried out by an expert Java programmer, using both the Android and iOS versions of the WideNoise code. Specifically, the code was reviewed to understand any processing and calibration stages that WideNoise use to convert the raw values obtained from the device microphone to the output DB values shown on the screen.

4.4 Test Results

Table 4.1 shows the results obtained in the sound chamber for each device, with Figure 4.4 presenting these in graphical format. As can be seen, while the majority of devices showed a stable measurement for each test, at lower values some fluctuation was observed on two devices (these cells are highlighted in red in Table 4.1).

In general there appear to be some significant discrepancies between the individual phones. At 70 dB(A) as measured on the reference device, the iPod Touch reported 83 dB while the Huawei Blaze reported 64 dB, a discrepancy of 19 dB between the two phones. While this difference between the individual device is large, individual devices tend to show fairly consistent errors across most of the measuring range.

Below 50 dB(A) the discrepancies between the phones and the reference meter are particularly pronounced. Importantly, during testing below 50 dB(A), it was found that very small changes of orientation of the mobile phones towards or away from the sound source, made large differences in apparent measured sound intensity. Some of the most wildly fluctuating measurements have been identified with a red background in Table 4.1. A possible explanation for this poor performance below 50 dB(A) is the actual physical characteristics of the microphones used in the mobile phones.

Equally, for values close to 100 dB(A) it appears that the sensitivity of the microphones is reduced due to saturation, indicating that 100 dB(A) is the maximum useful sound pressure. It is also worth

Figure 4.1: Noise calibration results in graphical format.

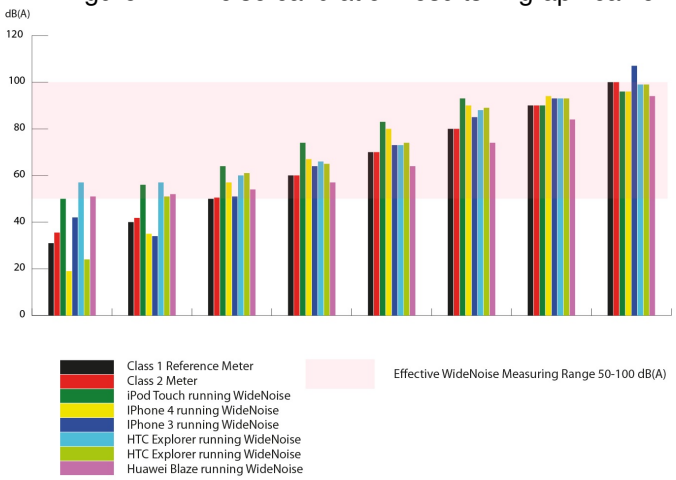

noting that during testing, the two identical HTC Explorer phones performed very similarly across the 50 - 100 dB(A) band, suggesting that by-model calibration is possible due to the similarity between instances of the same model.

4.4.1 Understanding the Code

Despite the fact that different models of mobile phone have different microphone characteristics a review of the source code revealed that WideNoise does not in fact employ a calibration algorithm as part of its code to correct for this factor. Instead, it uses a hard-coded sound profile based on an unknown device. This same profile is used in both the iOS and Android versions, regardless of the brand and model of the phone in use. Unfortunately, no details about the methods used to generate this profile are available.

4.5 Observations

From the results obtained above, it can be suggested that the range of 50 dB(A) to 100 dB(A) is the effective measuring range for the WideNoise application. In that range the level of discrepancy from the reference device was in the area of - 6dB(A) to + 14 dB(A). This provides a relatively useful indication of the general noise level.

However, it is important to note that without further calibration the current WideNoise data should be seen only as indicative. The predictability of the errors observed does suggest that it might be possible to carry out post-processing on the data to correct by model type. Indeed, a number of existing sound measuring applications for mobile phones do provide a means to calibrate and thus correct measurements on a per-model or per-device basis [HabitatMap and Lunar Logic Polska, 2011; Maisonneuve et al., 2010; Stevens, 2012]. As much of this information is open source, it may thus be possible to post-calibrate the readings generated by WideNoise. However, the number of devices for which detailed information is available is very limited. Additionally, the calibration process for additional devices is extremely time consuming (the process described above took 2.5 hours) and access to the sound chamber is limited as this is a shared facility. Thus such an approach may not be feasible, particularly given the increasing number of new Android devices released on a frequent basis and the relative rapidity with which devices become obsolete.

A second limitation identified as part of this review was the use by WideNoise of an unweighted

Sound Pressure Level (SPL) in dB rather than the A-weighted level used as standard. Again, other mobile phone applications such as NoiseTube [Maisonneuve et al., 2010; Stevens, 2012], NoiseSPY [Kanjo, 2010] and Ear-Phone [Rana et al., 2010] have demonstrated that it is technically feasible to implement an A-weighting filter on a mobile phone and this may be considered at a later stage of this project.

Finally, the experiments described above made use of white noise to ensure that the technical evaluation allowed for a range of diverse situations, and each test was repeated twice. It would have been preferable to repeat these measurement setups on a number of occasions. Additionally, it would be of interest to consider 'real-world' testing using target audio recordings to further understand the behaviour of selected devices under a variety of conditions. In both of these cases, however, the opportunity for further research is very much constrained by the availability of the sound chamber.

4.6 WideNoise 3.0

4.6.1 Story of the Application

WideNoise is a smartphone application to monitor noise levels around device. It is able to check the online map to see the average sound level of the area around as well as dedicated measurement points (see Figure 4.2). It was initially developed and maintained by WideTag Inc.[1].

Figure 4.2: WideNoise map view

WideNoise has a long history, from being a pioneering iPhone "spime" to being the showcase product of WideTag's OpenSpime protocol and WideSpime infrastructure. After being awarded the inclusion in the ADI Design Index 2011[2] and being cited as the Top 10 Internet of Things object of 2009[3] by the New York Times and Read Write Web, version 3.0 has been updated as a social

[1] http://www.widetag.com/

[2] http://www.adi-design.org/adi-design-index.html

[3] http://www.nytimes.com/external/readwriteweb/2009/12/08/08readwriteweb-top-10-internet-of-things-products-of-2009-74048.html

research tool within the EveryAware project.

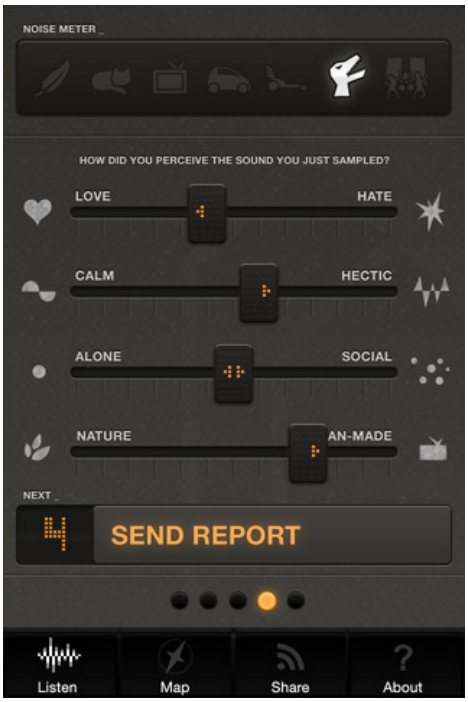

Figure 4.3: WideNoise perceptions slider view

WideNoise was completely redesigned in order to make it more like a professional tool. With the cooperation of the EveryAware project WideTag added some additional features like the slider to try and guess how much noise is there and the panel to add more details about the sampled noise itself (i.e., add perceptions as depicted in Figure 4.3, and tags).
All the raw data detections are being sent to the EveryAware REST server for collection. The application is free, its source is released with an open license.

4.6.2 Limitations

We list some limitation of the EveryAware system and WideNoise application. Most of them are typical for ubiquitous systems.

Lack of Data

An issue is the lack of geographical data. If both GPS and WiFi are not available, the geographic coordinates of the measurement can not be determined. Usually this sort of missing information can be restored with the help of IP address, but this is rather imprecise.

Distribution of Data

Despite the fact the active media campaign for the project has not started yet, some local and national media got interested in the project and made some articles. So the usage of the application worldwide is not uniform. The application is disseminated better where the project got an attention of media.
The usage of the application can not be controlled: The measurements are made whenever the users decide to use the application. So the frequency of measurements is not accessible.

Precision of Data

WideNoise supports almost all mobile phones using Android as operating system. This devices have different hardware (particularly speakers) manufactures and preferences. Some manufactures prefer to push loud or quiet noises to convince the user. The application could not be calibrated for all devices so the precision of the measurements is very difficult to estimate.

If the GPS-receiver is not available or does not receive a signal, the WiFi and / or GSM approximation can be used to localize the device. This localization service uses approximation algorithms and thus is not precise.

Chapter 5

Smartphone application design and implementation

The smartphone application mainly involves two elements (Fig. 5.1). The first element is the the user interface running inside the smartphone (i. e. the application) while the second element is the SensorBox itself.

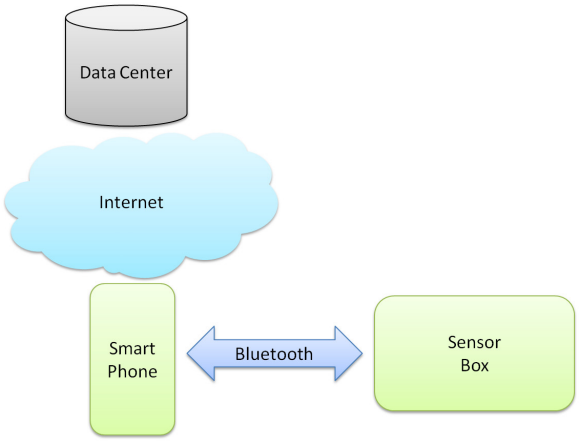

Figure 5.1: Smartphone application overview

At a first glance the application acts as a gateway between the sensor box and the data center where all readings are stored and further processed. From a certain point of view the sensor box can be seen as a hardware extension of the smartphone, containing all sensors that are needed for air quality measurement.

Even if limited by its computing power, the sensor box has its own intelligence and storage capability. From this point of view it cannot be seen simply as an extension of the smart phone, instead it is most similar to a data logger. Moreover the sensor box has an internal GPS receiver used to locate and time stamp the readings.

The Smartphone and SensorBox communicate using RFCOMM which is a profile of Bluetooth specification intended for serial communication (i. e. RS232 emulation). The Sensorbox starts to collect information from its sensor as soon as it is switched on. Data is stored inside a removable memory card (SD). When connected to the smartphone, the sensor box can provide live recordings to the application along with other information (e. g. the list of installed sensor and the status of the internal GPS). Live data are collected by the smartphone application and visualized to the user. They are also sent to the remote data center using the available network connection (Network Operator or Wireless).

The application also allows the user to send annotations alongside the readings (to allow the server

to correlate objective and subjective information). The annotations and collected data are stored on the smartphone memory if no connection is available, they are sent to the data center as soon as a working connection to Internet becomes available. This is exactly the same “Store’n’forward” paradigm used by electronic mail.

5.1 Communication protocols

5.1.1 SensorBox protocol

The first part of the communication protocol is the device “discovery”. There are two approaches to implement discovery of Bluetooth device:

- to implement SDP (Service Discovery Protocol);
- to use a convention in the device name.

The SDP is the most elegant way to implement service discovery mechanism in Bluetooth applications, but it is also more complex and has limitations in embedded platforms like Android (and even more for devices like the one used for the SensorBox). The use of a convention inside the name of the devices is a common solution to avoid all this problems, it is used in some commercial solutions (e. g. GPS receivers) and it has been chosen for this application. The convention is very simple: the box name is composed by a prefix and a suffix; the prefix is “SensorBox” while the suffix is an integer representing the serial number. (e. g. “SensorBox0001”) Using this simple convention, the smartphone application will be able to filter all the devices that are announcing themselves as SensorBox. If more than one sensor box is detected, the application will ask the user to select the one to be connected to. When the SensorBox is found, the application will connect to it using the SSP (Serial Port Profile) also known as RFCOMM. On top of this serial channel the application will send the string “%d” to the sensor box to request the live readings (GPS receivers, for example, will start sending data upon the connection is established, avoiding any form of control to the client application). When the start string is received by the SensorBox, it will start sending its readings using the CSV (Comma-Separated Values) format. Each line inside the CSV is a single reading that contains all the sensor values plus time-stamp information. The SensorBox generates a new record each second with the following fields:

1. Switch-on date in the format “DDMMYY”
2. Seconds since the switch-on
3. character “A” if the GPS is valid, “V” otherwise
4. latitude in degrees
5. character “N” for North
6. longitude in degrees
7. character “E” for East
8. the 10 sensor readings

The following dump is an example of data sent by the sensor box through the Bluetooth connection:

```
100712,080050.076,V,51.218238,N,4.417469,E,1.221,2.163,...,49.748
100712,080051.076,V,51.218288,N,4.417348,E,1.226,2.163,...,49.748
100712,080052.076,V,51.218345,N,4.417210,E,1.230,2.163,...,49.748
100712,080053.076,V,51.218425,N,4.417013,E,1.230,2.163,...,49.809
...
100712,080117.000,A,51.217525,N,4.420603,E,1.221,2.178,...,49.695
100712,080118.000,A,51.217525,N,4.420603,E,1.221,2.178,...,49.695
```

5.1.2 Server protocol

The application communicates with the Everyaware server using a REST (Representational State Trasfer) web service. The web services exposes two operations:

1. measurements submission;
2. map data retrieval.

The measurements submission operation is used to send sensor box readings to the server:

- URI: `/AirQualityApp/air/measurements/`
- Method: POST
- Content type: JSON
- Content encoding: GZIP

The JSON object is an array or records, each record contains the values of the a single measure. To optimize the transfer, the JSON object is compressed using GZIP algorithm.
The structure of the JSON object follows.

```
[
  {
     "uid": "047e362a5a277b8665fb67e7edfc1293",
     "device": "Android Phone",
     "session_id":"32892941a3ee568e812e498ae30d3e"
     "geo_coord": [
      "51.31178904285715",
      "37.785834"
      ],
     "timestamp": "1318581908",
     "co_1":"2.58",
     "co_2":"2.63",
     "co_3":"2.48",
     "co_4":"2.50",
     "no2_1":"3.11",
     "no2_2":"3.14",
     "voc_1":"4.00",
     "o3_1":"3.93",
     "temp":"19.7",
     "hum":"71",
     "user_data_1":"I feel happy about this",
     "user_data_2":"",
     "user_data_3":"",
     "user_data_4":"",
     "hash": "cMoGI1EsKKMMrzXvIuBEwzawwPtCqFBSWrXNWU0L0gs="
  },

  ...

  {
     "uid": "...",
     "device": "...",
     "session_id": "...",
     "geo_coord": [
      "...",
      "..."
      ],
     "timestamp": "...",
     "co_1":"...",
     "co_2":"...",
     "co_3":"...",
     "co_4":"...",
     "no2_1":"...",
     "no2_2":"...",
     "voc_1":"...",
     "o3_1":"...",
     "temp":"...",
```

```
      "hum":"...",
      "user_data_1":"...",
      "user_data_2":"...",
      "user_data_3":"...",
      "user_data_4":"...",
      "hash": "..."
   }
]
```

Data description:

uid a string that identifies univocally a device;

device device name;

geo_coord latitude and longitude expressed in degree (North/East);

timestamp time expressed as the number of seconds since “The Epoch” (01/01/1970);

hash this is an electronic signature of the request, calculated using a SHA256 HMAC with a shared secret; the HMAC is calculated on the JSON data with the “hash” key left blank;

co_X CO sensor number X value;

no2_X NO_2 sensor number X value;

o3_X O_3 sensor number X value;

voc_X VOC (Volatile Organic Compound) sensor number X value;

temp temperature sensor value;

hum humidity sensor value;

user_data_X additional information from the user input.

The second web service operation is used by the application to visualize the community map:

- URI: `/AirQualityApp/air`
- Method: GET
- Parameters: lat, lon, lat_delta, lon_delta, originator
- Content type: JSON

The parameters *lat,lon,lat_delta and lon_delta* are used to retrieve data belonging to a squared zone specified by a position and a range. The *originator* parameter is the *uid* of a device and is used to filter data collected based on its originator.
Example of request and response follows.

```
air/?lat=37.785792&lon=-122.406406&lat_delta=0.012447&
                                                lon_delta=0.013733
```

```
[
  {
     "id"="4edbe2fed31644904e00016f",
     "geo_coord": [ - 122.406417, 37.785834],
     "user_data": "blablabla",
     "avg_pollution":3.45,
     "timestamp":"1323033341"
  },
  ...
  {
```

```
    "id"="...",
    "geo_coord": [ ..., ...],
    "user_data": "...",
    "avg_pollution":...,
    "timestamp":"..."
  }
]
```

Description of the fields inside the response objects:

id unique identifier of the reporting device;

geo_coord coordinates of the report;

user_data additional user data;

avg_pollution an average indicator for the pollution;

timestamp the time expressed as number of seconds since “The Epoch”.

5.2 Working flow and layout

Once started, the application searches for bluetooth devices nearby. The search is done by identifying all devices whose name starts with the string `SensorBox`, this is a pretty simple alternative to the use of the more complex SDP (Service Discovery Protocol) and is used by some commercial devices (e. g. external GPS receivers).

The interface will show to the user a list of all sensor boxes during the detection. This process can be stopped anytime by the user, also note that the user can select the device as soon as it appears in the list, so he/she does not have to wait for the end of the discovery process.

After connected to the SensorBox, the application provides the general interface layout described in Fig. 5.2.

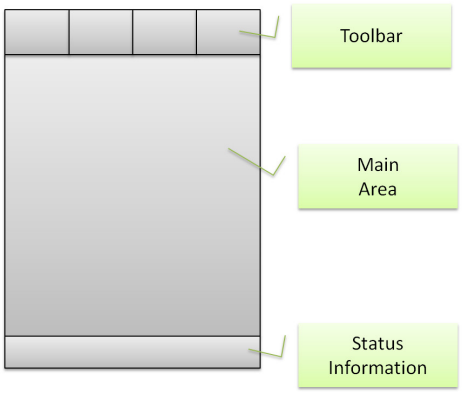

Figure 5.2: Smartphone application interface

The toolbar on top allows the user to switch between different views:

- the map;
- the graph;
- the sharing options;
- the SensorBox status.

The status bar is used to present useful information about ongoing connection to the SensorBox:

- status of the GPS inside the SensorBox;
- connection status with the SensorBox.

The main area content depend on the specific view selected by the user:

map - the main area displays the map with the position of the user, track information, waypoints, annotations and exposure feedback;

graph - the main area displays a live graph that visualize the raw readings from the sensors;

sharing options - the main area shows two buttons that can be used to login on Twetter and Facebook;

SensorBox status - provides detailed information about the SensorBox (e. g. list of the sensors).

All general information about the application are moved into the application menu (a standard Android UI element). The map is the central element of the user interface and has two display modes. The first mode shows user current position, his/hers track and annotations. From this mode it is also possible to provide/review annotations. The second mode displays the user position and all reading/annotation made by other people nearby.

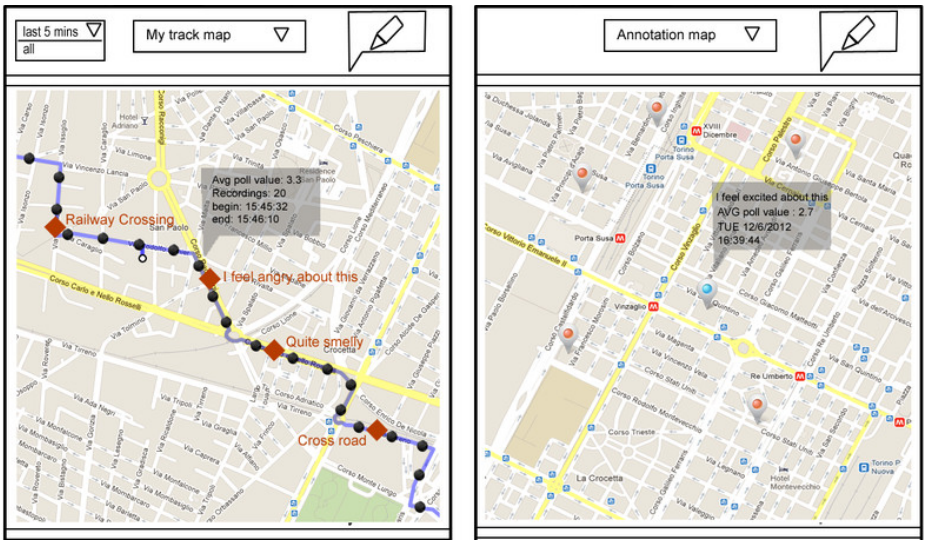

Figure 5.3: Map view prototype

Chapter 6

SensorBox evaluation and testing

6.1 Evaluation of sensorBox design

In this section some of the design decisions of the EveryAware SensorBox are evaluated. In the first subsection the gas flow through the sensor chamber is evaluated. In the second subsection, the sensor electronics are evaluated.

6.1.1 Gas flow through sensor chamber

The gas flow through the sensor chamber can have a significant influence on the obtained measurement results. In this subsection we evaluate both the actual measured gas flow through the sensor chamber and the air tightness of the sensor chamber. All measurements have been conducted on the two first EveryAware SensorBox prototypes equipped with fan. Both sensor boxes were equipped with a different mini fan because of availability reasons: SensorBox 1 was equipped with a Micronel F17LM-9 fan while SensorBox 2 was equipped with a Copal F17HA-05 MC fan. Both fans have the same specifications (See Table 3.2).

Initial sensor box

For the first experiment, the gas inlets of the EveryAware SensorBox prototypes were equipped with connectors which allow the usage of flexible tubes (Figure 3.3 left). The inner diameter of the used connectors is 4 mm.

During the flow measurements, both SensorBoxes were powered by attaching a USB cable directly to the Arduino Mega. To minimize the obstruction of the gas flow by the measurement device, a hot wire anemometer was used (the HTA anemometer of Höntzsch). At the gas inlet of each SensorBox, three measurements were executed during 30 seconds and the average values were calculated. During the measurements, the flexible tubes had been removed from the gas inlets. The measurement results are shown in Table 6.1.

Table 6.1: Gas flows measured (30 sec averages) with hot wire anemometers at gas inlets of first EveryAware SensorBox prototypes

Measurements	SensorBox 1	SensorBox 2
1	1.36 m/s	1.33 m/s
2	1.29 m/s	1.31 m/s
3	1.32 m/s	1.26 m/s
Average	1.32 m/s	1.30 m/s

The obtained measurement results are a flow of 1.32 m/s for SensorBox 1 and a flow of 1.30 m/s for SensorBox 2. As could be expected from two almost identical devices, the measurement results are close to each other. The average flow in liter/minute was calculated as follows:
The free surface of the gas inlet is: $\pi * r^2 = 3,14 * 0,002^2\,\mathrm{m}^2 = 1.256 \times 10^{-5}\,\mathrm{m}^2$.
This gives a flow in liter/minute of: $1.256 \times 10^{-5}\,\mathrm{m}^2 * 1.3\,\mathrm{m/s} = 1.63 \times 10^{-5}\,\mathrm{m}^3/\mathrm{s} = 0,016\,\mathrm{liter/s} = 0,98\,\mathrm{liter/min}$.
Since the sensor chamber of the first EveryAware SensorBox prototype has a size of around 0,54 liter, the time needed to refresh the sensor chamber is $\frac{0,54\,\mathrm{liter}}{0,98\,\mathrm{liter/min}} = 32\,\mathrm{s}$.
We consider a refreshment time of 32 seconds too long. Adaptations on the sensor box were required to enhance to flow.

Sensor box with enhanced flow

The theoretical highest flow which can be realized by fans is their free flow. According to the data sheets of the used mini fans, their free flow is 15 liter/minute. The measured gas flow at the gas inlet was 15 times smaller. As explained in section 3.1.2, the flow of a fan can be reduced significantly due to a pressure difference over the fan. For this reason, we tried to enhance the flow of the EveryAware SensorBox prototypes by removing obstacles from the path of the gas flow. The inlet tube of the SensorBoxes was replaced by a gas inlet pipe (Figure 6.1) with a much wider inner diameter (17 mm for pipe compared to 4 mm for tube). Also the gas outlet of the SensorBoxes was increased significantly to 21 mm diameter.

Figure 6.1: Sensor box equipped with wide tube on gas inlet (left) and increased size gas outlet (right)

The free surface of the gas inlet is now: $\pi * r^2 = 3.14 * 0.0085^2\,\mathrm{m}^2 = 2.269 \times 10^{-4}\,\mathrm{m}^2$
With the HTA anemometer of Hüntzsch a gas flow of 0.84 m/s was measured at the gas inlet of both sensor boxes. This produces a gas flow of: $2.269 \times 10^{-4}\,\mathrm{m}^2 * 0.84\,\mathrm{m/s} \approx 1.906 \times 10^{-4}\,\mathrm{m}^3/\mathrm{s}$ $\approx 0.1906\,\mathrm{liter/s} \approx 11.4\,\mathrm{liter/min}$.
The size increase of both the gas inlet and gas outlet was able to increase the gas flow though the sensor chamber with a factor 10. The calculated refreshment time of the sensor chamber is now $\frac{0.54\,\mathrm{liter}}{11.4\,\mathrm{liter/min}} = 2.84\,s$.

Air tightness of sensor boxes

We can calculate the air tightness of the EveryAware SensorBoxes by measuring also the gas flows at the gas outlets of the 2 sensor boxes. The results of those measurements are 0,47 m/sec for SensorBox 1 and 0,50 m/sec for SensorBox 2. This gives a flow at the gas outlets of respectively:
Outlet flow of SensorBox 1: $0.47\,\mathrm{m/sec} * \pi * 0,0105^2\,\mathrm{m}^2 = 1.63 \times 10^{-4}\mathrm{m}^3/\mathrm{s} = 9.76\,\mathrm{liter/min}$.

Outlet flow of SensorBox 2: $0.5\,\text{m/s} * \pi * 0.0105^2\,\text{m}^2 = 1.73 \times 10^{-4}\,\text{m}^3/\text{s} = 10.4\,\text{liter/min}$.

Based on those measurements we can calculate the losses of gas from the sensor chamber through small unwanted openings.

For SensorBox 1 are the losses: $\frac{11.4\,\text{liter/min} - 9.76\,\text{liter/min}}{11.4\,\text{liter/min}} = 14.4\%$

And for SensorBox 2: $\frac{11.4\,\text{liter/min} - 10.4\,\text{liter/min}}{11.4\,\text{liter/min}} = 8,8\%$

The observed losses (< 15%) are quite acceptable. A relatively large part of the gas (>85%) does reach the end of the sensor chamber. We expect the losses to be small enough to have all sensors in the sensor chamber exposed to the same gas mixture. Also the measurements indicate that the sensor chamber of SensorBox 2 has been made better air tight. A big part of this difference may be explained by the different kind of isolations strips used in both sensor chambers. In Figure 6.2 the isolation strips of SensorBox 1 (left) and SensorBox 2 (right) are depicted.

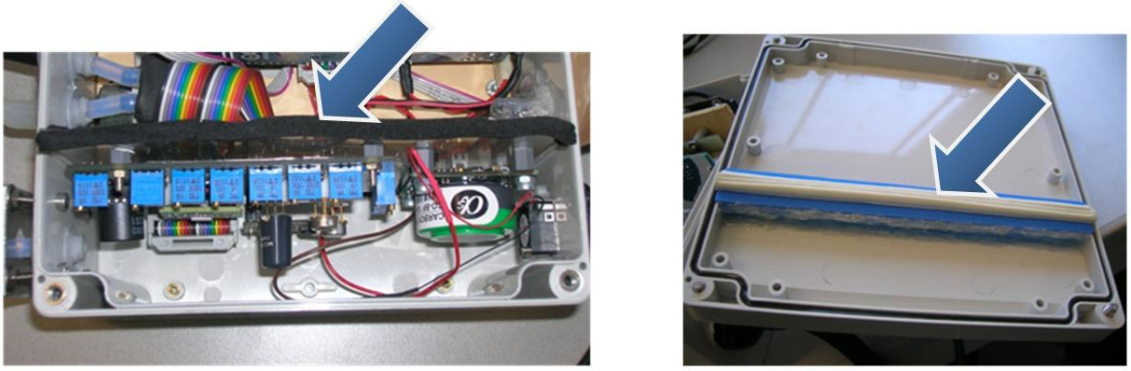

Figure 6.2: Isolation strips added to the sensor chamber of SensorBox 1 (left) and SensorBox 2 (right) to enhance the air tightness of the sensor chambers

6.1.2 Sensor electronics

The quality of the used sensor electronics has a large influence on the measurement results which can be obtained with low cost gas sensors. For this reason, both the sensor heater voltages and the noise on the sensor signals have been evaluated.

Sensor heater voltages

As explained in section 2.2, the temperature of the metal oxide sensor strongly influences both the sensitivity and selectivity of the sensor. Since the sensor temperature is determined by the power sent through the sensor heater element, and the resistance of the sensor heater element is quite stable, we can control the sensor temperature through the sensor heater voltage. It is important that each metal oxide gas sensor receives its correct heater voltage.

In Table 6.2, the required heater voltage and the measured heater voltage are given for each metal oxide gas sensor used in the EveryAware SensorBox. For some sensors, such as the E2V MiCS-2610 ozone sensor and the E2V MiCS-4514 NO_2 sensor in sensor box 1 (SB 1), the difference between the required and measured heater voltage are quite large. Most likely those wrong heating voltages have a negative impact on the sensor performance. Enhancements were applied to the electronics of the second EveryAware SensorBox prototype to avoid bad operating gas sensors due to wrong sensor heating. In Table 6.3, the measurement results of the heater voltages of the second EveryAware SensorBox prototype are presented. We can observe the measured heater voltages are now closer to the required heater voltages.

Table 6.2: Required versus measured heater voltages of first SensorBox prototypes

Sensor name	Required heater volt.	Heater volt. SB 1	Heater volt. SB 2
Figaro TGS 2201	5 V	4,75 V	4,82 V
E2V MiCS-5525 CO	2,4 V	2,26 V	2,32 V
E2V MiCS-4514 CO	2,4 V	2,38 V	2,28 V
E2V MiCS-4514 NO_2	1,7 V	1,40 V	1,60 V
E2V MiCS-2610 O_3	2,35 V	1,87 V	2,35 V
Applied Sensor AS-MLV VOC	2,7 V	2,64 V	2,7 V

Table 6.3: Required versus measured heater voltages of second SensorBox prototype

Sensor name	Required heater voltage	Measured heater voltage
Figaro TGS 2201	5 V	4,98 V
E2V MiCS-5525 CO	2,4 V	2,39 V
E2V MiCS-4514 CO	2,4 V	2,36 V
E2V MiCS-4514 NO_2	1,7 V	1.60 V
E2V MiCS-2610 O_3	2,35 V	2,32 V
Applied Sensor AS-MLV VOC	2,7 V	2,70 V

Noise on sensor signals

The EveryAware SensorBox should deliver measurement signals from all it's sensors with as little unwanted electronic noise on the sensor signals as possible. To get an idea of the electronic noise on the sensor signals, under realistic measurement conditions, both first EveryAware SensorBox prototypes have been placed inside a back pack with which a measurement walk was conducted through an urban environment. The measurement results of this walk are shown in Figure 6.3 and Figure 6.4.

In figure 6.3 the sensor signals of the E2V NO_x, Figaro diesel, Applied Sensors VOC and E2V ozone sensors in the two first prototypes of the EveryAware SensorBox are shown. Only the Figaro diesel sensor of SensorBox 1 picked up quite some noise on it's measurement signal.

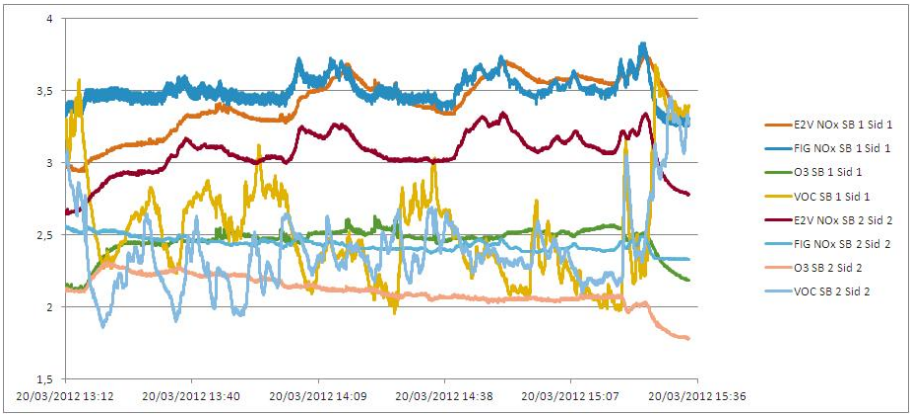

Figure 6.3: Sensor signals of NO_x, VOC and ozone sensors in the two first prototypes of the EveryAware SensorBox during a walk in urban environment

In Figure 6.4 the sensor signals of all used CO sensors (including Figaro gasoline) in the two first prototypes of the EveryAware SensorBox are depicted. A quite large amount of electronic noise is present on the measurement signal of all used E2V CO sensors (MiCS-5521 and MiCS-

5525). Also the Alpasense CO-BF sensors have a lot more noise on their measurement signal then expected.

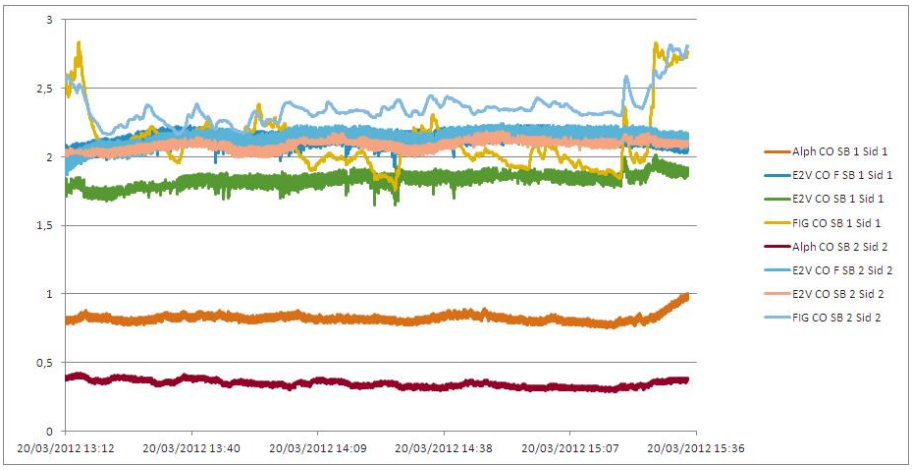

Figure 6.4: Sensor signals of all CO sensors in the two first prototypes of the EveryAware SensorBox during a walk in urban environment

The obtained measurement results have been compared against measurements under comparable measurement conditions with the same sensors but different sensor electronics. For the E2V sensors the E2V sensor evaluation board had been used and for the Alphasense CO-BF sensor home build electronics. During those measurements, significantly less noise was observed on the measurement signals. This indicates the noise on the measurement signals of the EveryAware SensorBox was not caused by the sensors but by the sensor electronics.

To cope with this issue, the sensor electronics of the second EveryAware SensorBox prototype has been enhanced for the reduction of electronic noise. The measurement results of a walk in urban environment with the second EveryAware SensorBox prototype are shown in Figure 6.5. We can observe a clear reduction of noise on the sensor signals compared to the first sensor box prototype.

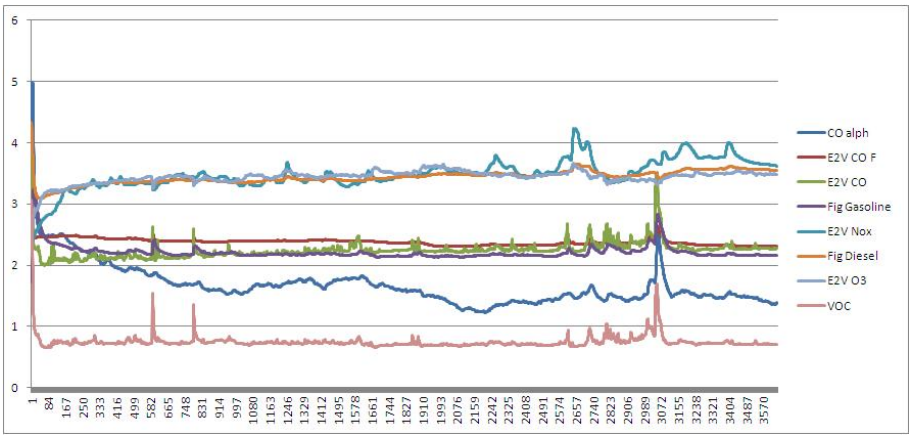

Figure 6.5: Sensor signals of gas sensors in the second EveryAware SensorBox prototype during measurement walk in urban environment

6.2 Calibration of the EveryAware SensorBox

6.2.1 Overview

An array of commercial low cost gas sensors has been mounted in the EveryAware sensor boxes. The main reason for the employment of low cost gas sensors is for densifying the sparse urban pollution monitoring mesh nowadays present.

On the other hand the utilization of low cost gas sensors has many drawbacks because they are not specifically designed for use in ambient air (low concentrations, complex mixtures) and are hence not very reliable. Evaluation of low-cost sensors for ambient air quality carried out in the Everyaware project showed that the low cost sensors need crucial counteraction for temperature or humidity drift and baseline drift by calibration.

To deploy the sensors in a complex and time-varying urban environment, with the task of monitor the concentration of harmful pollutants in an operational monitor network, strategies to counteract the above mentioned issues are needed in order to obtain reliable values from the gas sensors.

In the literature there are not many works that deal with the drift counteraction under ambient conditions, in comparison to studies in laboratory condition. Carotta et al. [Carotta et al., 2000] [Carotta et al., 2001] [Carotta et al., 2007] presented studies of few days measurement (3 up to one week) in an Italian city where they used tick-film gas sensors. They performed a field univariate calibration with least square methodology for NO_x and CO concentration estimation using as reference a governmental monitoring station. In their study the sensors showed good sensitivity but the stability of their counteraction method could not be evaluated because their measurement campaign was too short. Tsujita et al. [Tsujita et al., 2005] developed a gas sensor system (using commercial $TGS-2106$ from Figaro Engineering for diesel exhaust sensors [Figaro Engineering Inc.]) to be used as a sensing node to form a dense real-time environmental monitoring network. They proposed an auto-calibration method which aims to achieve a maintenance-free operation of the sensor network for NO_2 monitoring. To perform auto-calibration, first they have statistically studied the NO_2 concentration levels from four governmental monitors (around their sensor node) for a period of one year. They have found that when the NO_2 concentration in all the four stations went under $10ppb$ and the wind speed was in the order of 4 to $5m/s$, the NO_2 concentration was almost uniform in the whole study area. According to these studies they have adjusted the gas sensor system output to the average of the values measured at the four governmental monitor stations when all stations in the area simultaneously report concentrations less than $10ppb$ and the wind speed $> 4m/s$. Their method to counteract the long term baseline drift is limited to the study area and to the local meteorological conditions. If the weather does not match particular meteorological condition the zero base line drift could not be calculated and the auto calibration did not work. The short term drift, due to temperature and humidity changes, is counteracted by calculating the calibration curve in the laboratory with synthetic air mixtures in different humidity and temperature conditions. Kamionka et al. [Kamionka et al., 2006] presented a device (called “trisensors”) based on three sensitive tin dioxide (SnO_2) thick films. They performed first a calibration in laboratory with synthetic air of different humidity and temperature and then in field calibration using a reference analyzer measurements. To do that they have used a neural network (NN) to estimate NO_2 and O_3 levels. Their results are quite poor in term of sensitivity and stability (calibration has to be performed every few days). They justify these results with the low quality of the solid state devices used to measure the pollutant levels. De Vito et al. [De Vito et al., 2008] presented a low cost multi-sensor device based on seven solid-state sensors (5 gas sensors, one temperature and one humidity sensor) and a multivariate technique for on field calibration to estimate benzene levels. On field calibration was performed by means of a statistical sensor fusion algorithm, using a neural network (NN) and data from a governmental station as reference. De Vito et al. [De Vito et al., 2009] extended the previous work to the estimation of CO and NO_2. The sensing device and the measurement campaign are the same of the previous work. Also in this work they have used

NN regression technique to quantify the pollutant levels. They found that two weeks of training period for their NN was enough to have acceptable results for CO and NO_2 estimation tasks for 6 months.

In addition to drift problems, monitoring the health of any sensor network by detecting failing sensors is essential for a reliable functioning [Rajagopal et al., 2008]. A sensor may fail at any time, after which it reports incorrect measurements. Bad sensor detection from the sensors data is commonly based on models that try to identify which sensors have failed and when the fault occurred. A corrupted sensor could report values with implausible or plausible values. In the first case the fault could be easily and quickly recognized. In the latter case, fault detection is more difficult. Fault detection on low cost gas sensors has been tackled only in the case of laboratory condition or in the case of special chambers for industrial purpose, not in complex environment as in the case of air quality sensor network. Perera et al. [Perera et al., 2006] used recursive dynamic principal component analysis (RDPCA) to monitor the health of gas sensors (4 commercial Figaro and 3 CMOS based sensors) deployed in a gas chamber, which aims detecting filter damage in a industrial process. Pardo et al. [Pardo et al., 2000] in a laboratory test, used the correlation among the responses of five semiconductor thin films sensors to detect a possible malfunctioning of one sensors. The current flowing in each sensor was estimated from the current flowing in remaining ones by NN. In their experiments they used known mixtures of NO_2 (from 200 to $4000ppb$) and CO (up to $200000ppb$), quite far from the air quality standard. Moreover the fault due a long term drift has not been considered. Padilla et al. [Padilla et al., 2010] used principal component analysis (PCA) and Multiscale-PCA to identify and correct faulty sensors. Their method has been tested on a dataset composed of the response from an array of 17 gas sensors placed in a gas chamber for a period of 10 months.

6.2.2 EveryAware SensorBox Calibration Approach

In this section we introduce the basic idea of the EveryAware SensorBox (EA-SB) calibration. Considering the amount of EA-SBs that will be employed in the network (around 100 EA-SB) and the difficulties and cost to calibrate each sensor present in each EA-SB we have opted to employ a statistical approach to calibrate each EA-SB to a target pollutant directly in an outdoor environment (later referred as field-calibration) rather than calibrate each sensor in a laboratory.

The field-calibration has been inspired by the works of Carotta et al. [Carotta et al., 2000] [Carotta et al., 2001] [Carotta et al., 2007], Tsujita et al. [Tsujita et al., 2005], Kamionka et al. [Kamionka et al., 2006] and De Vito et al. [De Vito et al., 2008] [De Vito et al., 2009]. Short descriptions of these works are given in Section 6.2.1.

The basic idea relies in using supervised regression techniques to train a sensor array (based on low cost gas sensors, temperature and relative humidity sensors) to a target pollutant concentration values gathered by a more reliable and consequently more expensive monitor device (later referred as reference monitor). The field calibration is treated as multivariate supervised learning regression approach, where the inputs are the readings from the gas sensor array (S_k), temperature (T), relative humidity (rH) and the time stamp of the readings (t). The target are the pollutant concentrations as measured by reference monitors (P_{ref}).

Figure 6.6 shows a conceptual representation of the proposed field calibration approach. The upper part shows the inputs (**X**) and the target (y) of the training dataset; f is the model learned from the observed data. Squares represent observed variables and circles represent unknowns variables. The model f tries to capture the similarity existing between the fusion of the inputs (low cost gas sensors ($S_1, ..., S_k$), temperature (T), relative humidity (rH) and time (t)) and the pollutant concentrations gathered from reference monitor (P_{ref}). The bottom part shows the graphical model for the prediction phase, now the inputs are again the fusion of the low cost sensors information, and differently from the previous case the output is an estimated targeted pollutant

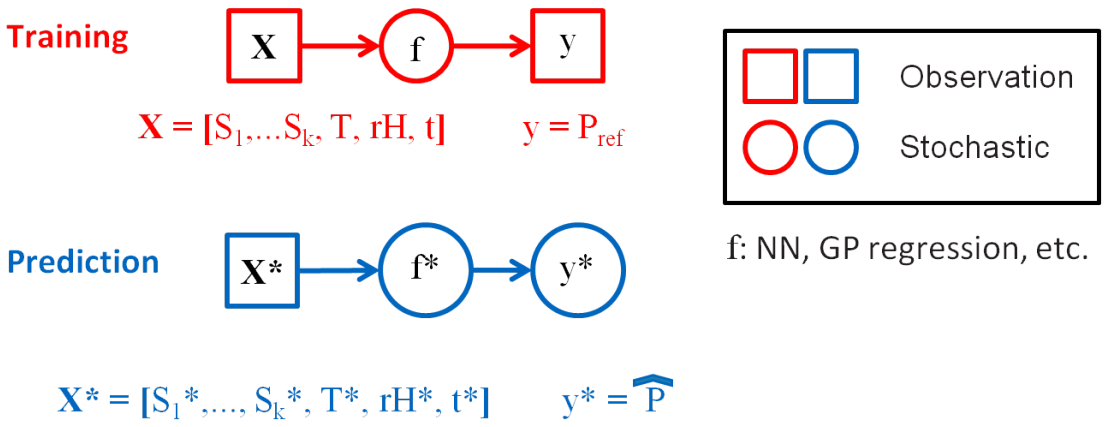

Figure 6.6: Conceptual representation of the training (top) and prediction (bottom) phases of the field calibration approach. Square variable are observed data and circles are unknown.

concentration ($\hat{P}$) based on the similarity between inputs and target learned in the training phase (also referred as learning phase). The calibration model could be computed with different non linear regression techniques. For example De Vito et.al [De Vito et al., 2008] [De Vito et al., 2009] used feed forward neural networks, here instead we will use Gaussian process regression (GP) [Rasmussen and Williams, 2006].

The proposed field calibration approach needs the employment of a reference monitor for the targeted pollutant in the training phase. The optimal length of the training period is not known a priori and depends on several variables, mostly related with the low cost sensor device used but also with other type of variables (for example locations were the sensors are deployed, pollutant concentrations and meteorological conditions). De Vito et.al [De Vito et al., 2009] have found for stationary application that a training period of two weeks is enough to achieve field calibration for a period of 6 months. At VITO we have obtained similar results in a study where sensor boxes have been deployed in the proximity of governmental monitor station. This approach tempts to address simultaneously three different issues related with the utilization of low cost sensor array:

- calibration;
- short term drift (daily gas sensor drift due to change in temperature and relative humidity between night and day);
- Baseline drift, or long term drift, due to gas sensor aging.

6.2.3 Calibration Strategies

In this section we describe and discuss in terms of effort (man power and facilities needed) two strategies (*stationary calibration* and *mobile calibration*) that will be evaluated in the following months to calibrate the EA-SBs.

Stationary Calibration

The first strategy is the most convenient from the point of view of man power effort and facilities required. The underlying idea of this strategy is to deploy the entire EA-SB in one location next to the reference device and simultaneously generate a calibration model for each EA-SB. Figure 6.7 (a) and (b) show a conceptual representation of the stationary calibration set-up and training model respectively.

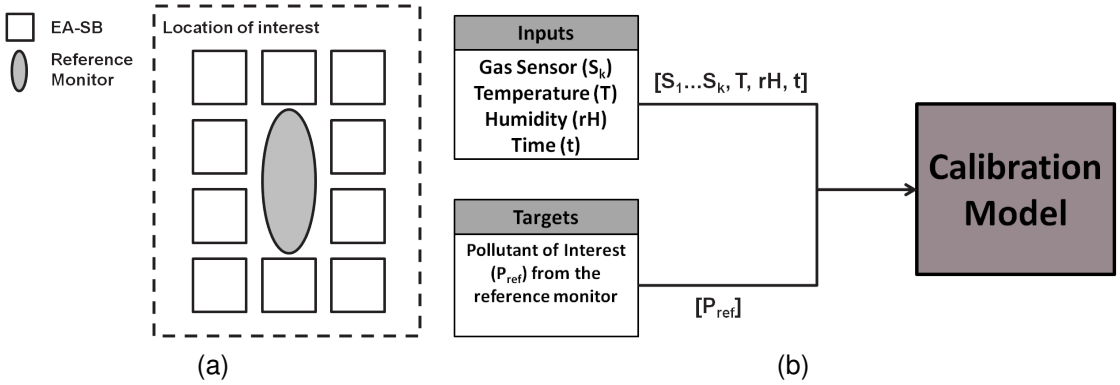

Figure 6.7: (a) Conceptual representation of the stationary calibration strategy. (b) Regression model to calibrate each EA-SB to a target pollutant.

This calibration strategy, as previously mentioned, is the most convenient in term of cost and facilities required. To compute all the calibration model, in principle only one reference monitor is required (two or more to avoid device malfunction). Moreover the stationary calibration strategy is almost a 100% stand alone set-up, avoiding thus great human effort during the training period. To the other hand, this strategy aims to simultaneously calibrate multiple EA-SBs in one locations and then deploy them in different measurement spots. At the best of our knowledge we do not know if this strategy works well, and if the calibration is location dependent or not. In only one work [De Vito et al., 2009] the author has suggested that probably the location is crucial in calibrating low cost gas sensors but results were not published. Anyway studies about this problem have not been reported yet.

One more aspect to consider is the location where to deploy the EA-SBs and the reference monitor during the training period. In order to give the opportunity to the calibration model to learn all the dynamics of the target pollutant, we suggest deploying the EA-SB and the reference monitor in a location that has similarities (i.e. morphology, traffic, etc.) with the locations where the mobile EA-SBs will be employed.

Mobile Calibration

The second strategy that will be investigated requires more human and facilities effort than the stationary calibration. The underlying idea of this strategy is to deploy few EA-SBs and one reference monitor in bags and employ humans to carry them around in the area of interest to collect the data necessary to build the calibration model. The computation of the calibration model is similar to the one presented in Section 6.2.2.

Figure 6.8 show an example of the mobile calibration set-up, in which several EA-SBs have been deployed in one backpack together with a reference monitor (in this case Micro-Aethalometer to measure black carbon), a GPS, a notebook and a mobile phone.

To compute all the calibration models, several reference monitors are required. Moreover this strategy requires great human effort during the training period (humans have to carry around EA-SBs and reference monitor for few hours every day and for a period of at least one week) to collect the data. To the other hand, the mobile calibration strategy should cope with the problem of location dependent calibration mentioned in the previous section. In this case, the calibration model should be able to learn the dynamics of the target pollutant during different days and different locations.

Figure 6.8: Example of the mobile calibration strategy set-up.

6.3 Evaluation of the SensorBox to conduct air quality measurements

In this section first we present the approach, the set-up and the efforts required to evaluate the calibration strategies described in Section 6.2.3. Then we introduce and discuss the utilization of different devices to be used as reference monitor in the framework of the EveryAware project and we present evaluation results for the chosen portable reference monitor device.

6.3.1 EveryAware SensorBox Calibration Evaluation Approach

To evaluate the calibration models strategies described in Section 6.2.3 we have opted to use the same set-up used in the mobile calibration strategy (Figure 6.8). One or a small group of persons will collect simultaneously data from several EA-SBs and from the portable reference monitor walking in an urban environment. This approach will be used to evaluate both the stationary and mobile calibration strategies (Section 6.2.3).

Figure 6.9 shows a conceptual representation of the evaluation strategy. The inputs of the calibration model (computed in the training phase for both stationary and mobile strategies) are the data gathered by the EA-SBs (gas sensor readings S_k, temperature T, relative humidity rH and time of the readings t) at different time from the ones used to compute the calibration models in the training phase.

Differently from the calibration case (Figure 6.6) the model generates an output ($\hat{P}$), which is an estimates of the target pollutant concentration, based on the similarities between the inputs and targets learned in the training phase (calibration). Moreover, the targets (readings from the portable reference monitor P_{ref}) are not inputs of the calibration model, but they will be used to evaluate the output of the calibration model ($\hat{P}$).

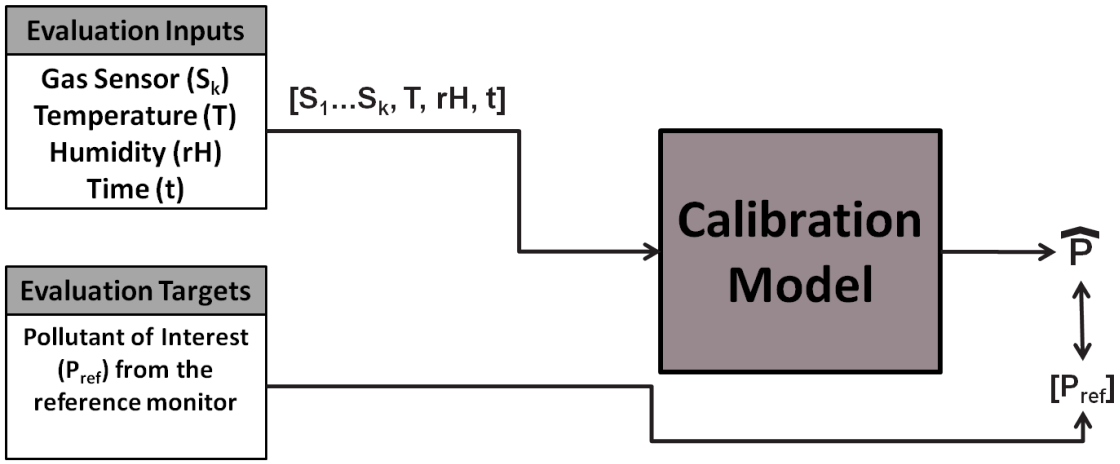

Figure 6.9: Conceptual representation of the evaluation model to evaluate the calibration of each EA-SB.

6.3.2 Target Pollutant and Reference Monitor

As described in Section 6.3.1 we treat the calibration of the EA-SBs as a supervised regression problem. In order to perform this task, the model needs, during the training phase, the values of a reference pollutant, in order to let the regression model to be able to learn the similarities between inputs (EA-SB) and targets (P_ref).

Considering the calibration strategies and the evaluation approach (described in Sections 6.3.1 and 6.2.2) the monitor to the reference pollutant has to be portable. Again, considering that in the framework of the EveryAware project, some citizens could carry around both the EA-SBs and the reference portable device, the portable monitor has to be easy to use. Moreover, considering that in the framework of the EveryAware project, the EA-SBs will operate in an urban environment the reference pollutant has to be a good indicator for the urban air quality.

Nitrogen dioxide (NO_2) is a regulated component of air pollution that is also used as an indicator of traffic-related air pollution (especially in area where the traffic is mostly predominated by diesel engine based) in health impact assessment and air quality management (Tonne et al. 2008). Similarly carbon monoxide (CO) dominate if the traffic related pollution is generated by gasoline engines and especially in developing countries where the air quality is affected by old engines and low petrol quality.

Unfortunately, portable reference monitor for those pollutants are not present in the market.

Other related traffic pollutants, not regulated yet, are ultrafine particles (particles having a diameter of less than 100 nm [Morawska et al., 1998], UFP) and black carbon (BC). The 90% of total UFP, in urban environment are generated by road vehicles [Harrison et al., 2011] [Pey et al., 2009]. Recently Janssen et al. [Janssen et al., 2011] have stressed that BC is a useful new indicator for the adverse health effect of traffic-related air pollution.

Portable monitors for those pollutants are present in the market. Portable devices that count the UFP number concentrations are:

- P-track from TSI Inc. [TSI Inc.] (Figure 6.10 (a))
- miniDiSC from Matter-Engineering AG [Matter - Engineering AG] (Figure 6.10 (b))
- Partector from naneos gmbh [Naneos particle solutions gmbh] (Figure 6.10 (c))
- NanoTracer and NanoMonitor from Philips Aerasense [Philips Aerasense] (Figure 6.10 (d) and (e))

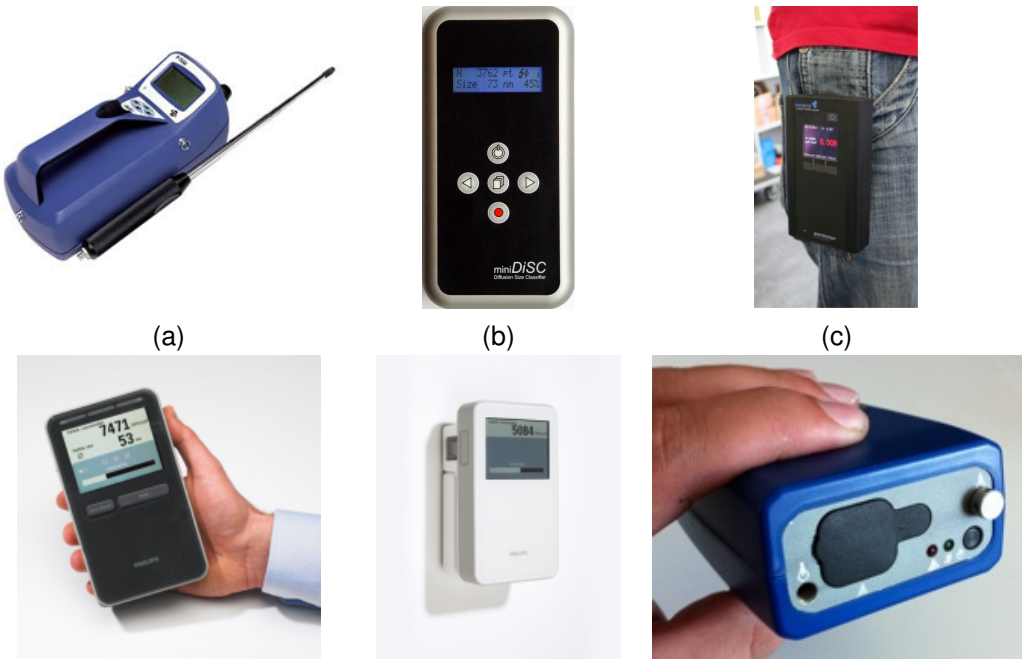

(a) (b) (c)

(d) (e) (f)

Figure 6.10: Portable monitors. (a) UFP counter P-track 8525 from TSI Inc. (b) UFP counter miniDiSC from Matter-Engineering AG. (c) UFP counter Partector from naneos gmbh. (d) UFP counter NanoTracer from Philips Aerasense. (e) UFP counter NanoMonitor from Philips Aerasense. (f) Black Carbon monitor Micro-Aethalometer AE51 from AethLabs.

and a portable device which measures BC concentration is:

- Micro-Aethalometer AE51 from AethLabs [AethLabs] (Figure 6.10 (f))

The cost of all those portable monitors are between 5000 to 10000 Euro. VITO has evaluated P-track, miniDisc, NanoTracer and Micro-Aethalometer using stationary and more precise (consequently more expensive and reliable) instrumentations as reference.

Partector has not been evaluated because the first device has been released in the market during summer 2012 and it has the same hardware of the miniDiSC. NanoMonitor from Philips Aerasense has similar specification than the other Philips Aerasense product NanoTracer.

Between the UFP monitors the P-track is the one that have shown better results. To the other hand, its operational principle is based on condensation and to work it needs a capsule of alcohol that has to be refilled every 6-8 hours.

After the evaluation of the devices (results are reported in Appendix) and considering the desired features that the portable device should have (portable, light, easy to use, minimal effort required and good indicator for urban air quality) we have opted to use the micro-Aethalometer Model AE51 as reference monitor in the framework of the EveryAware project. The choice is justified by the fact that this monitor is small and portable (250 g), has battery autonomy of up to 24 h, it requires minimal effort and measures BC concentration, which is a good indicator of traffic related pollution.

Micro-Aethalometer Evaluation

In this section we briefly describe the portable device (Micro-Aethalometer AE51 from AethLabs [AethLabs]) chosen as reference monitor in the framework of the EveryAware project. We also illustrate the minimal effort required and we conclude presenting a comparison of this device with one stationary and more precise monitor. The comparison has been performed by deploying two

Figure 6.11: Left: Micro-Aethalometer AE51 and the filter ticket. Right: installation of the filter ticket.

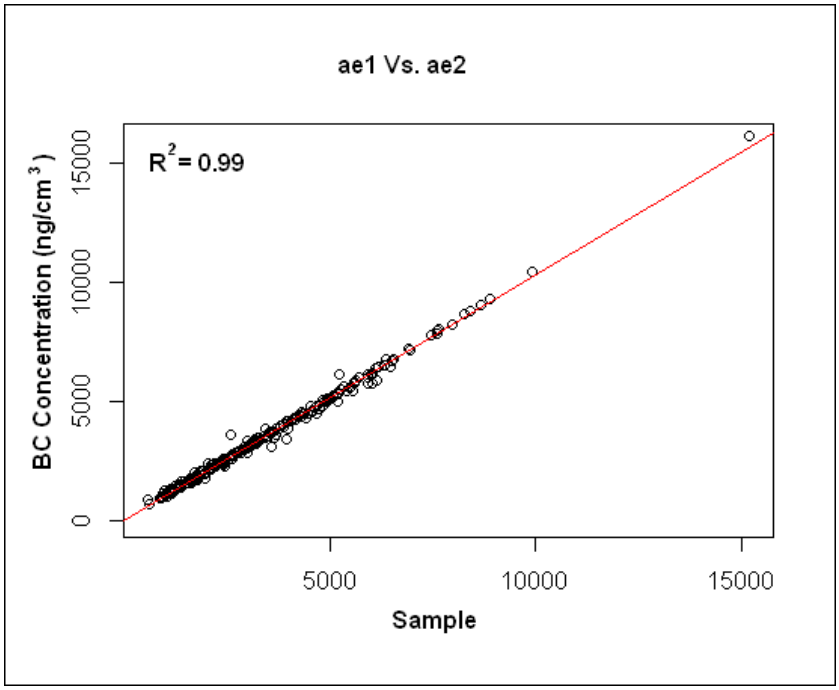

Figure 6.12: Comparison between two aethalometers deployed in an urban environment.

portable devices and the stationary monitor in an urban environment. The stationary monitor data, based on Multi Angle Absorption Photometer (MAAP), has been provided by the VMM, the Flemish agency which monitors air quality in Flanders.

The Micro-Aethalometer AE51 monitor is small and portable (250 g) and has battery autonomy of up to 24 h when the pump speed is set at a rate of 100 ml per minute. Inside there is a small Teflon-coated borosilicate glass fibre filter where BC-particles are captured. The aethalometer detects the changing optical absorption of light transmitted through this filter ticket. Every two days the filters have to be replaced. This action is fast and easy as shown in Figure 6.11. A noise reduction algorithm (ONA, [Hagler et al., 2011]) is applied to reduce the noise of the BC measurements.

In Figure 6.12 is plotted the scatter plot of two aethalometers, showing a good reproducibility of the measurements.

The left panel in Figure 6.13 shows the time series of the MAAP monitor (black) and the aethalometer (red), the right panel shows the scatter plot between the MAAP and the aethalometer showing a good correlation between the two measures ($R^2 = 0.76$).

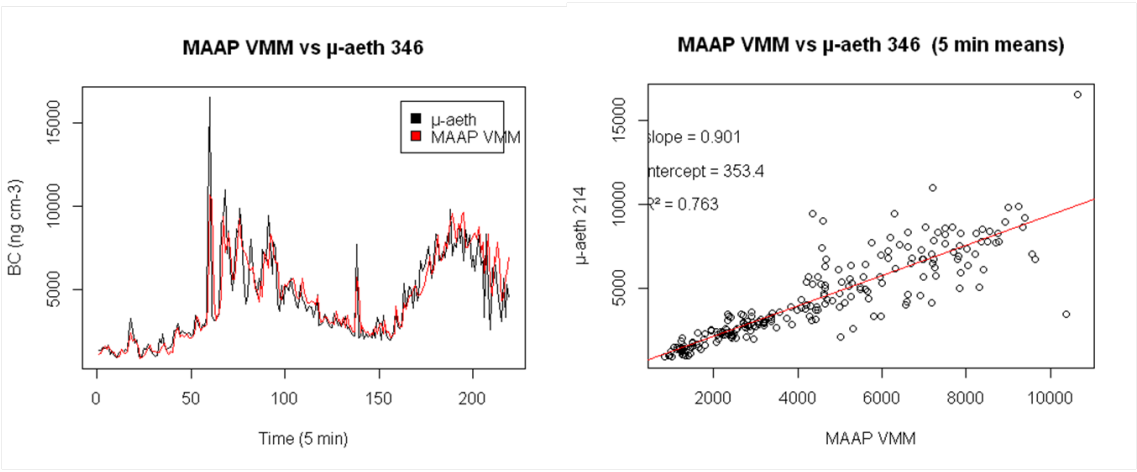

Figure 6.13: Left: time series of the MAAP (black line) and aethalometer (red line). Right: scatter plot between the MAAP and the aethalometer.

Appendix A

Evaluation of Portable Pollutant Monitors

A.1 UFP counter MiniDiSC

The MiniDiSC is a smaller version of the meDiSC (Matter Engineering Diffusion Size Classifier). Both instruments measure number concentrations and average size of particles in the size range $10 - 200nm$. The measurement principle is based on diffusion charging and current detection in two electrometers. The MiniDiSC is developed for personal exposure monitoring and for measurement networks.

The MiniDiSC was compared to the P-Trak. The P-Trak is also a mobile instrument for measuring particle number concentration (size range $20 - 1000nm$). The disadvantage of the P-Trak is that it need refills of isopropanol every 8 hours. In addition, the instrument needs to be positioned horizontally to prevent damaging of the optical part of the instrument.

A good correlation was found when comparing the MiniDiSC to the P-Trak. Figure A.1 shows the time profile for a short test (left) and the corresponding correlation plot (right). During the test, the instruments were used in a mobile application and stationary. The response of a passing vehicle during mobile use and of two passing vehicles during stationary use can be observed. Additional tests under conditions of high relative humidity confirmed the good correlation. However, the MiniDiSC showed to have a lower signal to noise ratio. When we received the instrument, it was previously tested by another potential customer. At the end of our tests a high corona voltage was observed. This can indicate a dirty corona wire and cleaning is then recommended. However the supplier only found a bad solder joint that should not have influenced the obtained results. Anyhow, the test results has to be considered in this perspective (worst case conditions).

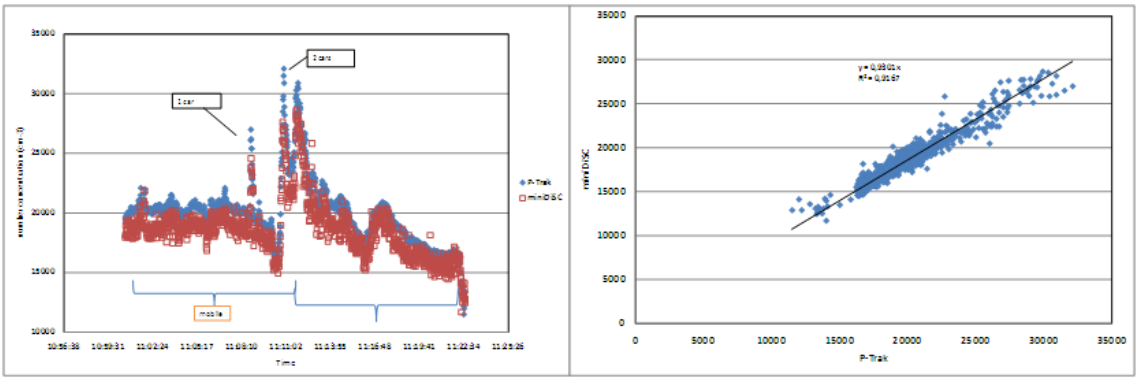

Figure A.1: Comparison of MiniDiSC and P-Trak

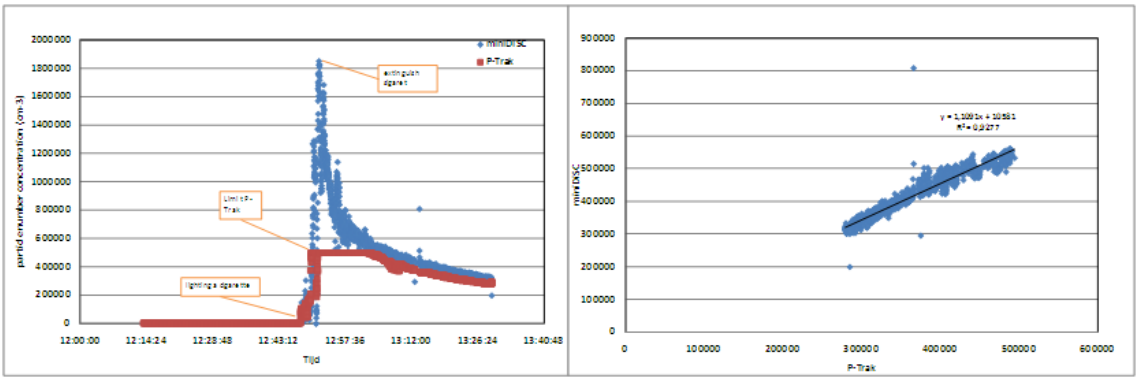

Figure A.2: Comparison of NanoCheck and P-Trak in glovebox

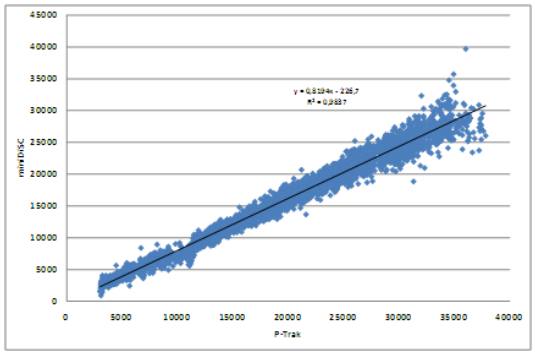

Figure A.3: Comparison of NanoCheck and P-Trak in glovebox at lower concentrations

When encountering very high concentrations, the MiniDiSC showed a better performance than the P-Trak. A test was performed in a glove box and ultrafine particles were generated using a cigarette. The very high concentrations could be measured by the MiniDiSC, whereas the P-Trak reached its known upper concentration limit at $500000 cm^{-3}$. At concentrations below 500000 a good agreement between both instruments was observed. The right plot of Figure A.2 shows the correlation of both instruments directly after extinguishing the cigarette.Figure A.3 shows the correlation at lower concentration during the same test set-up, when concentrations have decreased. At all of the tests, the instruments show a good correlation, however the estimated slope ranges between 0.82 and 1.1. The size distribution of the aerosol might affect the ratio, because both instruments have a different size range.

A.2 Micro Aethalometer

The Micro Aethalometer is a portable version of the Aethalometer. The aethalometer measures the attenuation of light through a filter as it loads over time. The change in attenuation gives the black carbon concentration as a function of time. Black carbon (BC) is a proxy for elemental carbon (EC) (formed by incomplete combustion) and a good correlation (site specific) was found between BC and EC. As such, even though the device does not measure ultrafine particles, it might still be useful to assess urban air quality related to traffic emissions.

The Micro Aethalometer contains a filter ticket. Depending on the black carbon concentrations it is exposed to, this ticket needs to be replaced daily to weekly.

The minimum time resolution of the instrument is one second. However, at low concentrations the signal to noise ratio is unacceptable. Therefore, a time resolution of 10 seconds to one minute is recommended. The instrument can be operated at 1 second base and concentrations can be

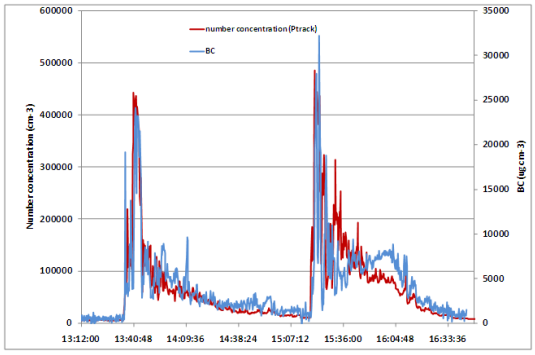

Figure A.4: Particle number concentration and BC during an experiment in hangar (on 25/2) with a diesel van using 15 second averaging time

recalculated on a larger integration time.

Figure A.4 shows the results of an experiment where both P-Trak and micro Aethalometer were used. The experiment was done in a hangar, where after a few minutes the engine of a diesel van was started to generate (representative) particulate emissions from traffic. The values were averaged on a 15 sec base to have good response time on one hand and a good signal to noise ratio on the other hand. Figure A.4 shows that both parameters show roughly a similar trend; however in some cases the ratio of the concentrations is different (e.g. after the second peak). This can be explained by the fact that particle number concentrations and black carbon are different parameters and their ratio depends on the size distribution and relative composition of the particles. During the same experiment, two micro aethalometers were used to compare different instruments and evaluate their correlation. The result is shown in Figure A.5. The figure shows that the correlation is better for 1-min averaging compared to 1 second averaging time. This is due to the higher noise at this time resolution.

Note that during the hangar experiment AE209 was placed on a shaking apparatus (performing a rotating movement) to check if movement has an effect on the readings of the instrument. Time trends (Figure A.5) show no significant difference in noise between both instruments, except from some individual peaks. No comparison between both instruments was made under normal conditions (without shaking apparatus) during this experiment. However the slope of the correlation plot is similar as observed in previous experiments done at VITO (between 0.9-1.1).

The hangar experiment was repeated using only two micro aethalometers. A higher concentration range was reached compared to the previous experiment. The aethalometers show a good correlation ($R^2 = 0.97$) over the entire concentration range.(Figure A.6).

Some preliminary tests were performed to check the effect of relative humidity (rH) on the BC readings. The experiment was performed in a room where a humidifier was installed. During the experiment two aethalometers were used: one with a new filter (AE 209) and another with a loaded filter ticket (AE 214). Figure A.7 shows that rH has an effect on the noise of the BC signal. There seems to be a slight effect on average concentration; however, it cannot be concluded how large this effect is. It is possible that the spraying of the humidifier has a larger influence, creating droplets, compared to the rH values. BC readings are more influenced by rH when using a loaded filter compared to a new filter ticket.

A.3 Correlation of BC and UFP with other traffic related pollutants

In the hangar experiment, similar trends for BC were observed as for UFP (number concentrations). However, the UFP measurement device is able to measure at a shorter time resolution as compared to the BC micro aethalometer, therefore correlation on a $1s$ base was not good. Figure

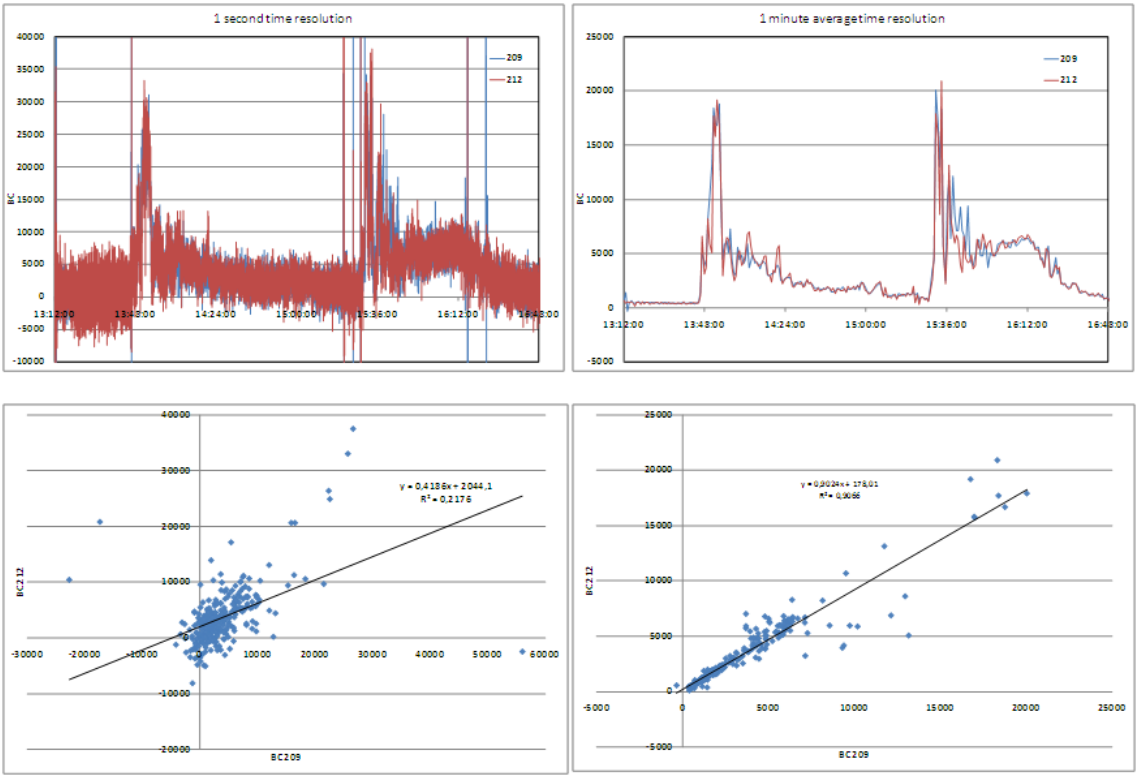

Figure A.5: Comparison of 1 second (left) and 1 minute (right) averaging time for BC measurements using micro aethalometers: time trends are given in the figures on top; corresponding correlations are shown in the figures below.

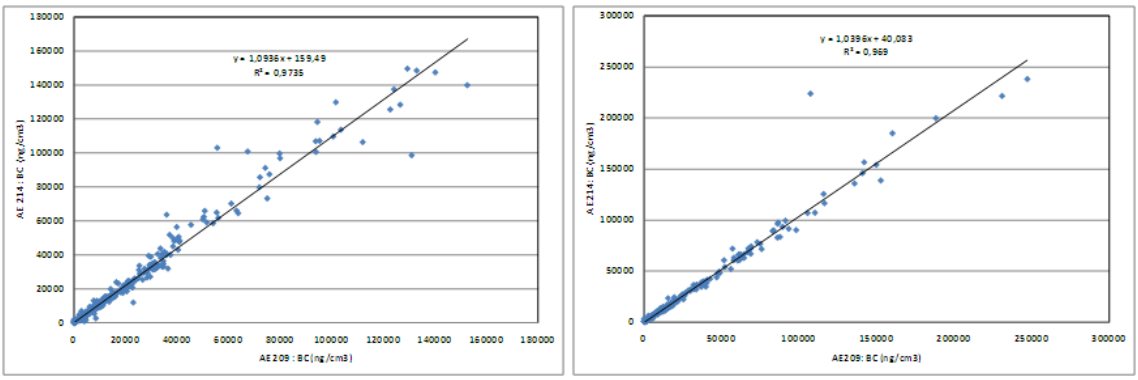

Figure A.6: Comparison of two micro aethalometers using 10 second averaging time during two experiment in a hangar with a diesel van.

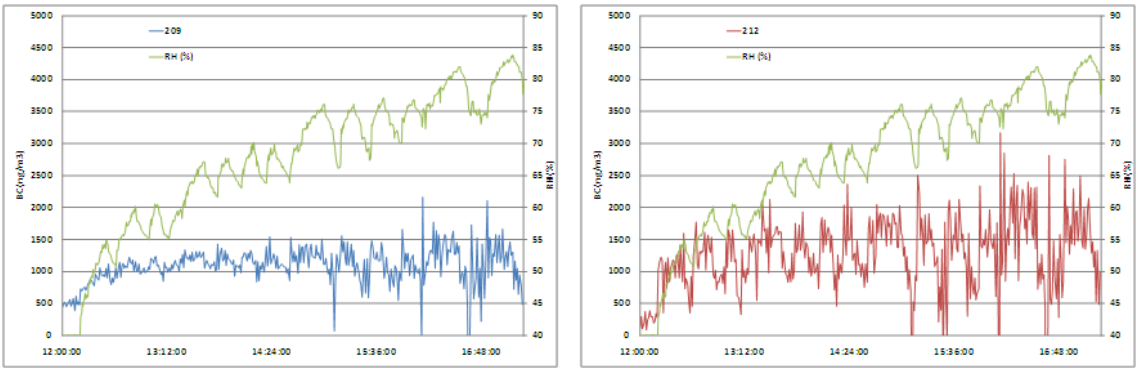

Figure A.7: Effect of rH (%) on BC readings using new (left) and loaded (right) filter ticket.

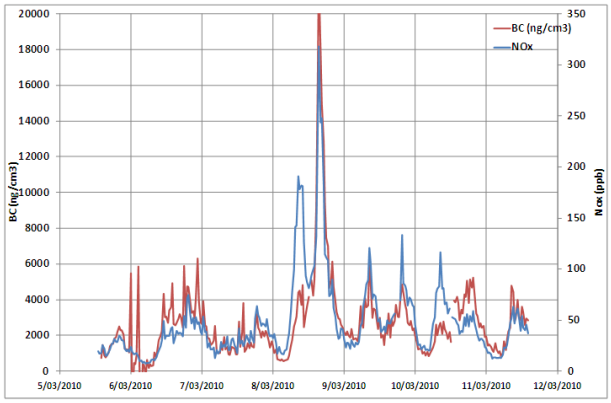

Figure A.8: BC and NOx concentrations near Districthuis in Antwerp.

A.8 shows the NOx and BC profile in a street in Antwerp. Similar trends for both pollutants can be observed. Figure A.9 shows one day for which also data for ultrafine particle number concentration (PNC) were available (measured with SMPS with particle range of $10 - 500nm$).

Corresponding correlation plots are shown in Figure A.11. A good correlation between all these pollutants is observed.

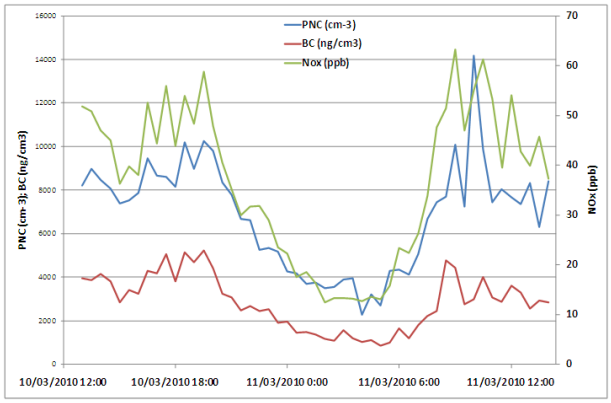

Figure A.9: UFP, BC and NOx concentrations during 1 day .

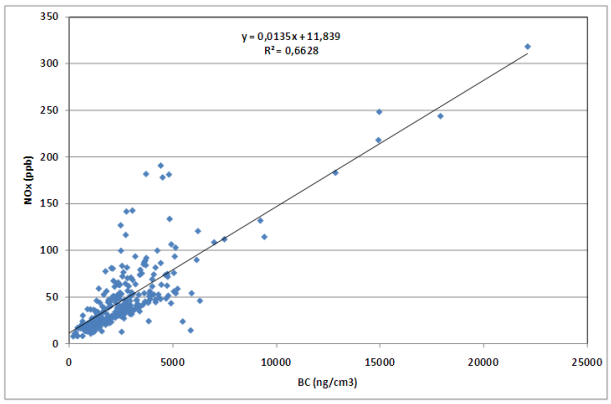

Figure A.10: correlation of NOx and BC during measurement campaign in Antwerp.

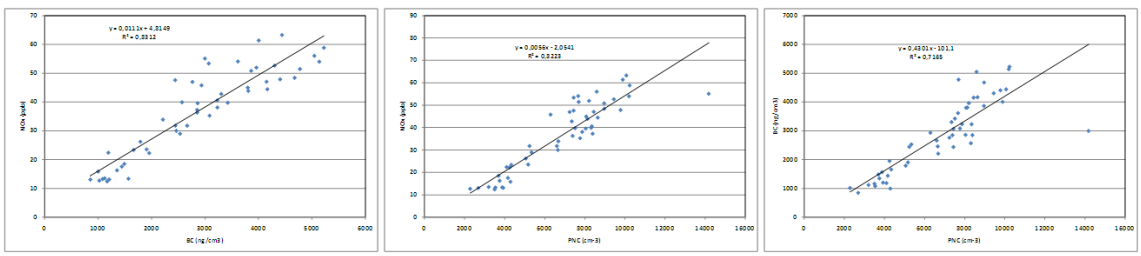

Figure A.11: Correlations plots for NOx, BC and PNC for a 1 day comparison in Antwerp.

Bibliography

AethLabs. http://www.aethlabs.com.

PM Aoki, RJ Honicky, A Mainwaring, C Myers, E Paulos, S Subramanian, and A Woodruff. A vehicle for research: using street sweepers to explore the landscape of environmental community action. In *Proceedings of the 27th international conference on Human factors in computing systems*, CHI '09, pages 375–384, New York, NY, USA, 2009. ACM. ISBN 978-1-60558-246-7.

Arduino open-source electronic prototyping platform. http://www.arduino.cc/.

MC Carotta, G Martinelli, L Crema, M Gallana, M Merli, G Ghiotti, and E Traversa. Array of thick film sensors for atmospheric pollutant monitoring. *Sensors and Actuators B: Chemical*, 68(1 - 3):1 – 8, 2000.

MC Carotta, G Martinelli, L Crema, C Malagu, M Merli, G Ghiotti, and E Traversa. Nanostructured thick-film gas sensors for atmospheric pollutant monitoring: quantitative analysis on field tests. *Sensors and Actuators B: Chemical*, 76(1 - 3):336 – 342, 2001.

MC Carotta, M Benetti, E Ferrari, A Giberti, C Malagu, M Nagliati, B Vendemiati, and G Martinelli. Basic interpretation of thick film gas sensors for atmospheric application. *Sensors and Actuators B: Chemical*, 126(2):672 – 677, 2007.

Cirrus Research plc UK. Glossary of noise measurement terminology. http://www2.ph.ed.ac.uk/acoustics/teaching/acoustics/CirrusTerminology.pdf.

Custom Sensor Solutions. Model 1402 static potentiostat. URL http://www.customsensorsolutions.com/m1402.html.

S De Vito, E Massera, M Piga, L Martinotto, and G Di Francia. On field calibration of an electronic nose for benzene estimation in an urban pollution monitoring scenario. *Sensors and Actuators B: Chemical*, 129(2):750 – 757, 2008.

S De Vito, M Piga, L Martinotto, and G Di Francia. Co, no2 and nox urban pollution monitoring with on-field calibrated electronic nose by automatic bayesian regularization. *Sensors and Actuators B: Chemical*, 143(1):182 – 191, 2009.

E Dons, LI Panis, M Van Poppel, J Theunis, H Willems, R Torfs, and G Wets. Impact of time-activity patterns on personal exposure to black carbon. *Atmospheric Environment*, 45(21):3594 – 3602, 2011.

European Parliament and Council. Directive 2002/49/EC of 25 June 2002 relating to the assessment and management of environmental noise. *Official Journal of the European Communities*, L 189(45):12–26, 2002. ISSN 0378-6978. URL http://ec.europa.eu/environment/noise/directive.htm.

Everyaware Project. Everyaware Widenoise. http://cs.everyaware.eu/event/widenoise, 2012.

Figaro Engineering Inc. http://www.figarosensor.com.

HabitatMap and Lunar Logic Polska. AirCasting. http://aircasting.org, 2011.

GSW Hagler, TLB. Yelverton, R Vedantham, ADA. Hansen, and JR Turner. Post-processing method to reduce noise while preserving high time resolution in aethalometer real-time black carbon data. *Aerosol and Air Quality Research*, 11:539 – 546, 2011.

RM Harrison, DCS Beddows, and M Dall'osto. Pmf analysis of wide-range particle size spectra collected on a major highway. *Environmental Science and Technology*, 45(13):5522 – 5528, 2011.

Institute for Software Integrated Systems. Maqumon: Mobile air quality monitoring network. URL http://www.isis.vanderbilt.edu/projects/maqumon.

International Organization for Standardization. Acoustics – Description, measurement and assessment of environmental noise – Part 2: Determination of environmental noise levels. ISO 1996-2:2007, 2007. URL http://www.iso.org/iso/catalogue_detail?csnumber=41860.

NAH Janssen, G Hoek, M Simic-Lawson, P Fischer, L van Bree, H ten Brink, M Keuken, RW Atkinson, HR Anderson, B Brunekreef, and FR Cassee. Black carbon as an additional indicator of the adverse health effects of airborne particles compared with pm10 and pm2.5. *Environ Health Perspect*, 119(12):1691 – 1699, 08 2011.

A Juszkiewicz and B Kijak. Traffic-Generated Air Pollution with Volatile Organic Compounds in Krakow and its Environs. In *Polish journal of environmental studies*, volume 12, pages 49–56, 2003. number = 1.

M Kamionka, P Breuil, and C Pijolat. Calibration of a multivariate gas sensing device for atmospheric pollution measurement. *Sensors and Actuators B: Chemical*, 118(1 - 2):323 – 327, 2006.

E Kanjo. Noisespy: A real-time mobile phone platform for urban noise monitoring and mapping. *Mob. Netw. Appl.*, 15(4):562–574, August 2010. ISSN 1383-469X. doi: 10.1007/s11036-009-0217-y.

KickStarter. The air quality egg kickstarter page, a. URL http://www.kickstarter.com/projects/edborden/air-quality-egg.

KickStarter. The sensor drone kickstarter page, b. URL http://www.kickstarter.com/projects/453951341/sensordrone-the-6th-sense-of-your-smartphoneand-be.

N Maisonneuve, M Stevens, and B Ochab. Participatory noise pollution monitoring using mobile phones. *Information Polity*, 15(1-2):51–71, August 2010. ISSN 1570-1255. doi: 10.3233/IP-2010-0200. URL http://soft.vub.ac.be/Publications/2010/vub-tr-soft-10-14.pdf.

Matter - Engineering AG. http://www.matter-engineering.com.

L Morawska, S Thomas, N Bofinger, D Wainwright, and D Neale. Comprehensive characterization of aerosols in a subtropical urban atmosphere: particle size distribution and correlation with gaseous pollutants. *Atmospheric Environment*, 32(14 - 15):2467 – 2478, 1998.

Naneos particle solutions gmbh. http://www.naneos.ch.

Noise Meters Limited. Type or class of a sound level meter. http://www.noisemeters.co.uk/help/faq/type-class.asp.

M Padilla, A Perera, I Montoliu, A Chaudry, K Persaud, and S Marco. Fault detection, identification, and reconstruction of faulty chemical gas sensors under drift conditions, using principal component analysis and multiscale-pca. In *Neural Networks (IJCNN), The 2010 International Joint Conference on*, pages 1 –7, july 2010.

M Pardo, G Faglia, G Sberveglieri, M Corte, F Masulli, and M Riani. Monitoring reliability of sensors in an array by neural networks. *Sensors and Actuators B: Chemical*, 67(1 - 2):128 – 133, 2000.

A Perera, N Papamichail, N Barsan, U Weimar, and S Marco. On-line novelty detection by recursive dynamic principal component analysis and gas sensor arrays under drift conditions. *Sensors Journal, IEEE*, 6(3):770 – 783, 2006.

J Pey, X Querol, A Alastuey, S Rodriguez, JP Putaud, and R Van Dingenen. Source apportionment of urban fine and ultra-fine particle number concentration in a western mediterranean city. *Atmospheric Environment*, 43(29):4407 – 4415, 2009.

Philips Aerasense. `http://www.aerasense.com`.

J Polak and N Hoose. Message - mobile environmental sensing system across grid environments, 2009.

Radiation watch. `http://www.radiation-watch.org/`.

R Rajagopal, X Nguyen, SC Ergen, and P Varaiya. Distributed Online Simultaneous Fault Detection for Multiple Sensors. In *Proceedings of the International Conference on Information Processing in Sensor Networks (IPSN 2008)*, pages 133 – 144, Washington, DC, USA, 2008.

RK Rana, CT Chou, SS Kanhere, N Bulusu, and W Hu. Ear-Phone: An End-to-End Participatory Urban Noise Mapping System. In *IPSN 2010: Proceedings of the 9th ACM/IEEE International Conference on Information Processing in Sensor Networks (April 12-16, 2010, Stockholm, Sweden)*, pages 105–116, April 2010. ISBN 978-1-60558-988-6. doi: 10.1145/1791212.1791226.

CE Rasmussen and CKI Williams. *Gaussian Processes for Machine Learning*. MIT Press, MIT Press, Cambridge, MA, 2006.

S Santini, B Ostermaier, and R Adelmann. On the Use of Sensor Nodes and Mobile Phones for the Assessment of Noise Pollution Levels in Urban Environments. In *INSS2009: Sixth International Conference on Networked Sensing Systems (17-19 June, 2009, Pittsburgh, PA, USA)*, pages 1–8. IEEE, 2009. ISBN 978-1-4244-6313-8. doi: 10.1109/INSS.2009.5409957.

M Stevens. *Community memories for sustainable societies: The case of environmental noise*. PhD thesis, Faculty of Science, Vrije Universiteit Brussel, Brussels, Belgium, June 2012. URL `http://brussense.be/phd-matthias`.

The Air Quality Egg. The air quality egg wiki. URL `http://airqualityegg.wikispaces.com/`.

TSI Inc. `http://www.tsi.com`.

Wataru Tsujita, Akihito Yoshino, Hiroshi Ishida, and Toyosaka Moriizumi. Gas sensor network for air-pollution monitoring. *Sensors and Actuators B: Chemical*, 110(2):304 – 311, 2005.

UCL. The anechoic chamber. `http://www.ucl.ac.uk/psychlangsci/research-facilities/anechoic-chamber`, a.

UCL. Ear institute. `http://ucl.ac.uk/ear`, b.

Vishay VBPW34 photodiode. `http://www.vishay.com/docs/81127/vbpw34fa.pdf`.

Vlaamse Milieumaatschappij. Jaarverslag lozingen in de lucht 1990-2009. Technical report, VMM, 2009.

P Völgyesi, A Nádas, X Koutsoukos, and Á Lédeczi. Air quality monitoring with sensormap. In *Proceedings of the 7th international conference on Information processing in sensor networks*, IPSN '08, pages 529–530, Washington, DC, USA, 2008. IEEE Computer Society. ISBN 978-0-7695-3157-1.

Widetag. About Us. `http://www.widetag.com/about-us/`, 2012.

World Health Organization. Transport, environment and health. WHO regional publications. European series 89, WHO, 2000.